# Abstract

| | |
|---|---|
| Title of Dissertation | Functionalization of Consumer Grade Fabric for Atmospheric Carbon Capture Proposal |
| Dissertation Directed by | Professor Mohamad Al-Sheikhly, Department of Materials Science and Engineering |

Primary amines contribute to a well-studied mechanism for capturing carbon dioxide ($CO_2$) from the atmosphere. This thesis describes two approaches to grafting amine-containing monomers to three commercial-grade fabrics: polyethylene terephthalate, high-density polyethylene, and Nylon 6. Initially, two monomers, allylamine and butenylamine, were chosen and evaluated for their sorbent capabilities. After confirming the selected monomers chemisorb $CO_2$, six novel copolymers, composed of each of the three fabrics grafted with one of each monomer, were synthesized through two unique single-step fabrication processes, though both rely on free radical addition polymerization of the monomers. In the first synthesis method, electron beam radiation created the free radicals necessary for grafting. In the second, nitroxide and peroxide chemical initiators created the free radicals. This chemically initiated graft polymerization process resulted in qualitatively successful monomer attachment. All copolymers synthesized via radiation-induced graft polymerization achieved greater grafting with butenylamine compared to allylamine, likely given the closer proximity of the primary amine to the radical on the latter's structure. Characterization of $CO_2$ capacity, the figure of merit for sorbency, revealed not only that the majority of the grafted amines likely reacted to adsorb $CO_2$, but secondary physical mechanisms also contribute to $CO_2$ abstraction. Additionally, economic and environmental analyses were conducted to quantitatively determine the viability of the manufacture of consumer-grade $CO_2$ sorbents, both in terms of cost and $CO_2$-capturing efficacy.

# Functionalization of Consumer Grade Fabric for

# Atmospheric Carbon Capture Proposal

Sean Cook, Pablo Dean, Eli Fastow, Patrick Ott, Jonathan Wilson, Hojin Yoon

May 1, 2020

Advisory Committee
Professor Mohamad Al-Sheikhly, Chair
Professor John Cumings
Dr. Zois Tsinas
Professor Luz Martinez-Miranda
Professor Robert Briber
Professor Alison Flatau

# Acknowledgements

# Contents

# List of Tables

# List of Figures

# 1  Introduction

Climate change remains one of the most daunting modern issues. With fossil fuel usage beginning in the Industrial Revolution, atmospheric carbon dioxide ($CO_2$) levels have steadily risen. Currently, the global mean marine surface $CO_2$ levels measure at roughly 410.88 parts per million (ppm) according to the National Oceanic and Atmospheric Administration [42]. For comparison, before widespread industrialization in the 19th century, $CO_2$ concentrations remained fairly constant at 280 ppm [65]. While research continues today to fully elucidate the effects of rising $CO_2$ levels on human and natural systems, the Intergovernmental Panel on Climate Change's 4th assessment report directly tied rising $CO_2$ levels to global warming [40]. This mechanism for global warming is well understood through the greenhouse gas effect. Greenhouse gases in the atmosphere, such as $CO_2$, absorb infrared radiation emitted from the earth. In turn, these gases raise the temperature of the earth's surface and the troposphere. However, the effects of rising $CO_2$ levels are not limited to the greenhouse gas effect. The current literature offers a bleak assessment that implicates higher atmospheric concentrations of $CO_2$ as the cause of extreme weather patterns, rising ocean levels, ocean acidification, and ice cap melting. Additionally, since the largest use of energy in the temperate latitudes can be attributed to space heating and cooling, the rising Earth surface temperatures are responsible for an additional energy burden. All these impacts severely impair the habitability of the earth, and with the continued rise in carbon dioxide levels, these problems will only worsen and reach irreversible levels.

Thus, climate change is a pressing issue that requires a multifaceted response. The various approaches being considered include improved energy efficiency, development of alternative energy sources, and $CO_2$ capture and storage. With over 60 % of carbon emissions stemming from power and industrial sectors in 2005, the demand for fossil fuel alternatives has grown [40]. Similarly, carbon capture technologies have sought to mitigate carbon emissions from these large point sources. Even if carbon capture methods were 90 % efficient and implemented at every large point source facility, over 50 % of $CO_2$ emitted globally would remain unaffected [63]. Additionally, few companies have

been willing to implement carbon capture solutions due to economic feasibility concerns. Therefore, the direct capture of atmospheric carbon dioxide is appealing as it promises the capture of $CO_2$ from delocalized sources in addition to large point sources, yet the technology remains relatively unexplored.

Carbon capture technologies generally rely on the development of specialized materials with properties that allow the material to either absorb or adsorb $CO_2$. Absorption refers to the diffusion of carbon dioxide into the bulk of the material, while adsorption refers to the binding of carbon dioxide to the surface of the material. Sequestration is achieved through either chemical or physical mechanisms. The two mechanisms have benefits and shortcomings that are highly dependent on the specific material. Chemical carbon capture involves the formation of a chemical bond between the material and $CO_2$, usually achieved with a functional group that is reactive with $CO_2$. On the other hand, physical mechanisms are based on highly specific geometries that allow for the trapping of $CO_2$ within the bulk of the material [60].

For carbon capture technology, there exist specific criteria the technology must meet in order to be effective. The main criteria are high carbon dioxide capacity and rapid kinetics, which maximizes the material's cost-effectiveness. Additionally, the material must selectively react with or physically trap carbon dioxide rather than other compounds. Otherwise, the efficiency of the system will be severely limited. Other considerations include the robustness of the material to withstand physical and chemical deterioration and the cost-efficiency for sequestering $CO_2$. This cost-efficiency of the material for removing carbon dioxide should be around \$ 100 per ton of carbon dioxide absorbed [24]. Lastly, the material must allow for the removal of captured $CO_2$ such that the functionalized material is regenerated and available for further $CO_2$ capture. In order to meet this criteria, Team Capture proposed to functionalize commercial-grade fabrics to adsorb $CO_2$ from the atmosphere.

In order to create a novel fabric with the potential of widespread use, Team Capture used Polyethylene Terephthalate (PET), High-Density Polyethylene (HDPE), and Nylon-6. Since PET is the most commonly used polyester and HDPE and Nylon are also

commonly used, successful modifications to these fabrics that do not affect the morphology of the fibers will allow carbon capture technology to be adapted to a wide range of markets. Thus, the potential market for carbon capture technology will be drastically extended. Similarly, by targeting commercial fabrics, consumers will be offered the ability to participate in the fight against climate change. Unlike large industries, consumers are more likely to pay the additional cost of the modified fabrics for the sake of combating global warming. While large industries take on large expenses to implement new technology, the cost would also be split among all the consumers who purchase the product.

The literature review below will evaluate the feasibility of several of the most prevalent sorbents. The optimal sorbent for this project is one that has reasonable flexibility, low cost, high regenerability, and high capacity and selectivity for $CO_2$. This project has focused on evaluating the carbon capture density of fabrics modified using radiation-induced and chemically initiated graft polymerization with three amine-based monomers. The monomers were selected based on their ability to both capture $CO_2$ and attach onto the fabrics examined. Adsorption experiments were run to examine the ability of each monomer to capture $CO_2$. Monomers were then grafted onto fabrics both through irradiation and chemical activation. We examined the modified fabrics for the presence of amine groups using spectroscopy and also evaluated their respective $CO_2$ capacities with adsorption experiments. The steam stripping of loaded fabrics was not evaluated because it is beyond the scope of the project. A simplified economic and environmental analysis was then carried out to determine where improvements need to be made in order for the process to be feasible.

## 2 Review of Literature

This review of $CO_2$ sorbents intends not only to detail existing methods reported in literature, but also evaluate their efficacy. The primary figure of merit for carbon dioxide sorbents is $CO_2$ capacity, typically measured in units of moles of $CO_2$ captured per either mass of sorbent or mole of sorbent [24, 29, 17]. Another important metric of sorbent

quality is its reusability, measured in the decay in $CO_2$ capacity as a function of sorption-desorption cycles [33].

This literature review divides $CO_2$ sorbents into two categories based on their primary means of absorbance: either physisorption or chemisorption. Each of these two categories are further divided into subcategories that detail additional literature describing the development of specific material systems. Each of these material systems works best for specific applications. While many of the systems reviewed in section 3 are developed for large point $CO_2$ sources, such as factories or power plants, our work seeks to develop a novel $CO_2$ sorbent and a simple fabrication process ideal for local point sources.

## 2.1 Reported Methods of Chemisorption

### 2.1.1 Resins

Recently, researchers have evaluated commercial adsorbent resins, such as HP2MGL, as a method for economically viable air capture. While the resins do not directly capture $CO_2$, they exhibit high chemical and physical stability and therefore serve as a support for the adsorbent. As aforementioned, studies focus on amine-based monomers as adsorbents because of their ability to reversibly attach to $CO_2$. The resins are impregnated with amines by dissolving the monomer, adding the resin, and drying the adsorbent-resin complex. In a recent study, this process lasted over a day for 2 grams of resin to be generated; however, multiple samples could be generated simultaneously. Additionally, diffusion additives were added to increase the rate of impregnation by the amines. Further research is required to determine if the amines would detach from the resin over time or under certain conditions. Wang et al. tested the $CO_2$ adsorption capacity of PEI-impregnated HP2MGL under various conditions to determine the ideal loading capacity. The percentage of amines occupied by $CO_2$ significantly decreased when the amines surpassed 60 % of the total weight of the solid [54].

Furthermore, the study researched the impact of both moisture and $O_2$ in the air on $CO_2$ adsorption capacity. Initially, the rise in humidity causes an increase in the maximum $CO_2$ adsorption capacity because the water vapor reacts with the amine-$CO_2$

complex to regenerate primary amines for further reaction. However, as humidity further increases, the capacity steadily decreases, likely due to water interfering with $CO_2$ and competing for the same adsorption sites. Similarly, $O_2$ competes with $CO_2$ for adsorption sites and additionally oxidizes several regions of the amine-based molecules. This oxidation negatively impacts the adsorption capacity because it renders several of the adsorption sites unusable for future trials after the first desorption, reducing the capacity by approximately 13.5 % from 2.13 to 1.84 mmol $CO_2$ adsorbed per gram of adsorbent [54].

Research conducted by Akingbogun et al. investigated the adsorption capacity of ion-exchange resins (IERs) functionalized with a primary amine group. IERs are organic polymer substrates that behave as media for the exchange of ions due to their porous surface area and purifying nature. Specifically, Akingbogun et al. tested a cross-linked polymeric resin containing benzyl amine groups in several conditions, such as at varying levels of humidity and concentrations of $CO_2$. At $CO_2$ levels comparable to that of the atmosphere, the resin was able to adsorb $CO_2$ at a rate of 1 mol/kg of resin, with the rate of adsorption rising to 3.4 mol/kg at conditions of moderate humidity [1]. The primary benefits of resins include their low cost, capability to desorb 99 % of adsorbed $CO_2$ at relatively low temperatures, and effectiveness at atmospheric $CO_2$ concentrations. The main weakness of resins for carbon capture lies in its relatively low peak $CO_2$ capacity, which is further reduced after the first adsorption cycle due to the presence of O2. The effects of these external factors on $CO_2$ adsorption, as well as the cost of fabricating the adsorbent complex relative to maximum $CO_2$ capacity and rate of adsorption, must be evaluated and considered.

Due to the similar capture mechanism of amine-impregnated resins and amine-grafted fabrics, knowledge of resins can guide the optimization of grafting methods. Specifically, the critical amine loading (found to be 60 % for HP2MGL) must be determined for the relevant fabrics and monomers to accurately determine maximum adsorption capacities. The grafted amines are likely to have much lower loading due to the lack of bulk absorption; however the number of attached amines would have a more immediate impact on the

adsorption capacity. Furthermore, the effect of oxygen and humidity should be considered when evaluating adsorption capacity due to their drastic impact. In order to be viable, the cost of the graft polymerization must be less than that of making adsorbent-resin complexes or the product must have a superior capacity per gram of adsorbent.

### 2.1.2  Fiber-Based Sorbents

For the ultimate purpose of synthesizing $CO_2$ sorbents, the use of synthetic fibers as the main substrate for polymerization has also been investigated in prior studies. A common mechanism by which to attach monomers onto fibers involves radiation-induced graft polymerization. The procedure consists of irradiating the substrate with ionizing radiation so as to break a covalent bond, thus forming a molecule with a lone, unpaired electron in one or more of its atoms' outer shells; these highly unstable atoms are called free radicals, as shown in Figure 1. When in close contact with the monomer of choice, a free radical formed on the substrate is expected to spontaneously react with the double bond, thus beginning a chain mechanism through which the monomer becomes radical-ized, thereby attaching to other monomers of its own kind in the process [38]. Only when two free radicals form a covalent bond is the polymerization terminated.
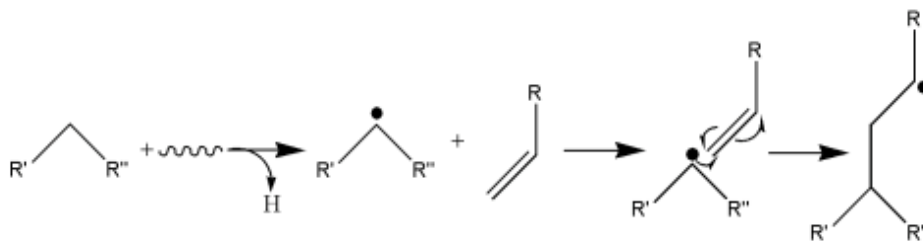


Figure 1: Radiation-induced graft polymerization

The studies conducted by Yang et al. and Wu et al. both employed a straightforward grafting technique that is both quick and regenerative (Yang, Li, Chen 2010; Wu, Chen, Liu 2014). When preparing to graft 2-propen-1-amine (allylamine) onto polyacrylonitrile (PAN), the substrate was irradiated, washed with DI water, and mixed with two initiators, ammonium persulfate $((NH_4)_2S_2O_8)$ and sodium bisulfite $(NaHSO_3)$ [58]. The purpose of these initiators, which form free radicals under extreme heat, is to rad-

icalize the monomer so that it can form a covalent bond with the radicalized substrate. Similarly, in the case of grafting polyethylenimine (PEI) onto polypropylene fiber, ammonium ferrous sulfate $((NH_4)_2SO_4)(FeSO_4)(6\,H_2O)$ was used as a free radical initiator [56]. Because both of these processes require the use of an initiator, a smaller margin for error exists for efficiently grafting the desired monomer onto the substrate of choice. Due to potential unwanted free radical reactions that may occur when introducing a set of unstable initiators, other monomers must be researched for their spontaneity in reacting with radicalized substrate. Grafting aside, the $CO_2$ adsorption capacities exhibited by the aforementioned fiber-based amine monomers show promise. Allylamine grafted onto PAN showed a 6.22 mmol $CO_2$/g capacity while PEI grafted onto polypropylene adsorbed 4.8 mmol $CO_2$/g [58, 56]. In addition, another study that did not employ radiation-induced grafting but instead incorporated a wet impregnation method found that PEI-coated glass fibers adsorbed 6.29 mmol $CO_2$/g [32]. However, this study used a cross-linking resin to prepare the substrate and monomer, which would likely render the material too stiff for a commercial-grade fabric. Grafting and impregnating $CO_2$ adsorbents onto fibers is a promising method by which to manufacture materials that renewably capture ambient $CO_2$.

Additionally, the $CO_2$ adsorption capacity of amine-grafted activated carbon fiber has been tested at various levels of humidity [6]. However, said sorbent made use of a highly microporous structure not commonly found in consumer-grade fabrics. The adsorption capacity of amine-grafted consumer-grade materials remains an unexplored topic that will offer new knowledge regarding the viability of consumer-scale carbon capture.

## 2.2 Reported Methods of Physisorption

### 2.2.1 Zeolites

Zeolites comprise a broad category of aluminosilicate ceramics typically used in catalysis and separation science [37]. In a zeolite sorbent, aluminum, silicon, and oxygen form a tetragonal cage where the partial negative charge on the aluminum atoms enables the stabilization of positively charged groups that attract $CO_2$ through coulombic interactions

with the partial negative charge on the oxygen atoms [45, 59, 7]. Synthetic zeolites typically exhibit well controlled pore sizes on the order of single nanometers, enabling size-based filtration of molecules in atmosphere [37].

Utilizing zeolites for the purpose of $CO_2$ sequestration has remained an active area of research since the 1970s through today. In a notable advance, Dr. Youngmin Cho of the Korea Railroad Research Institute modified zeolites to capture $CO_2$ at ambient temperatures with the addition of lithium hydroxide to the aluminosilicate frameworks [7]. Adding the lithium hydroxide provided the positively charged group that engages in physical interactions with atmospheric $CO_2$. Cho et al modified 13X zeolite pictured in figure 2. In a similar vein, Dr. Arnost Zuka achieved similar adsorption properties by introducing magnesium oxide to thin film zeolites [64].
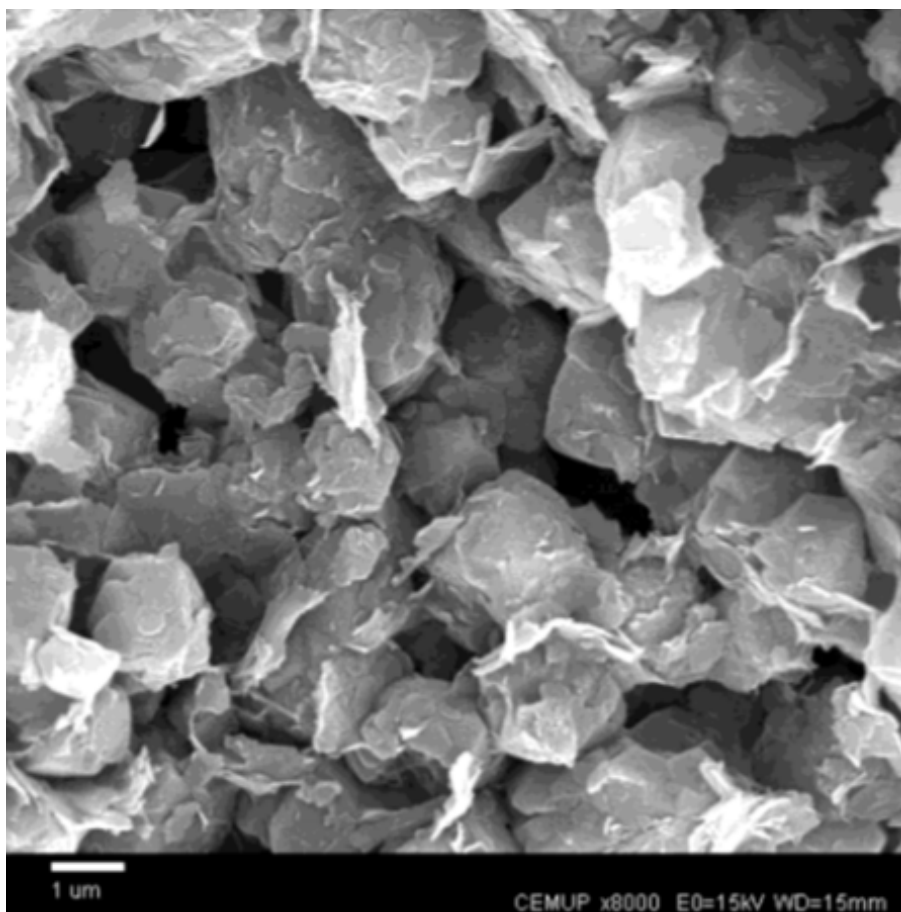


Figure 2: Surface features of Zeolite 13X powder under SEM with 8000x magnification [5].

Further work by Dr. Hauchhum mapped chemical properties and kinetics of $CO_2$

capture by zeolite sorbents. That work found that the $CO_2$ adsorption process matches Le-Chatlier's principles with respect to partial pressure, where an increase in pressure increased the amount of $CO_2$ adsorbed. However, raising the temperature decreased the amount of $CO_2$ adsorbed, potentially indicating an entropic driving force opposing adsorption [21].

### 2.2.2 Monolithic Carbon Fiber

In response to a demand for structurally resilient sorbents for large-point source $CO_2$ sequestration several industries adopted highly porous monolithic carbon fiber sorbents, a well developed technology. These sorbents capture $CO_2$ through intermolecular dispersion interactions between the carbon fibers and the $CO_2$ molecules trapped in small pores [51, 48]. Monolithic carbon fiber consists of continuous carbon fiber—synthesized through the pyrolysis of an ultra high molecular weight polymer fiber—secured in a polymer matrix [51]. The most effective carbon fiber sorbents exhibit a 12 wt. % $CO_2$ capacity.

# 3 Single-Step Synthesis of Atmospheric $CO_2$ Sorbents through Radiation Induced Graft Polymerization on Commercial-Grade Fabrics

## 3.1 Introduction to Radiation Induced Graft Polymerization (RIGP)

Primary or secondary amines enable a well studied reaction that binds atmospheric $CO_2$ to a substrate. These functional groups are stable at high temperatures, humidity, and pressure [36, 16, 11, 52]. Thus, chemisorbent systems commonly use the reaction driven by primary or secondary amines to capture $CO_2$. This mechanism exhibits an enthalpy of reaction of –80 kJ(mol$^{-}$1) at 40 °C and is therefore energetically favorable [39]. The primary or secondary amine adsorption reaction with $CO_2$ follows two steps: $CO_2$ binds to an amine to form a zwitterion, then another amine deprotonates the zwitterion, as

indicated in equation 1 and 2 [39].

$$RR'NH + CO_2 \leftrightarrow RR'N^+HCOO^-$$ (1)

$$RR'N^+HCOO^- + RR'NH \leftrightarrow RR'NCOO^- + RR'N^+H_2$$ (2)

Figure 3 depicts the arrow pushing mechanism of this reaction. As shown in Figure 3, the reaction begins with a nucleophilic attack on the carbon in $CO_2$ and concludes with a deprotonation of the resulting zwitterion.
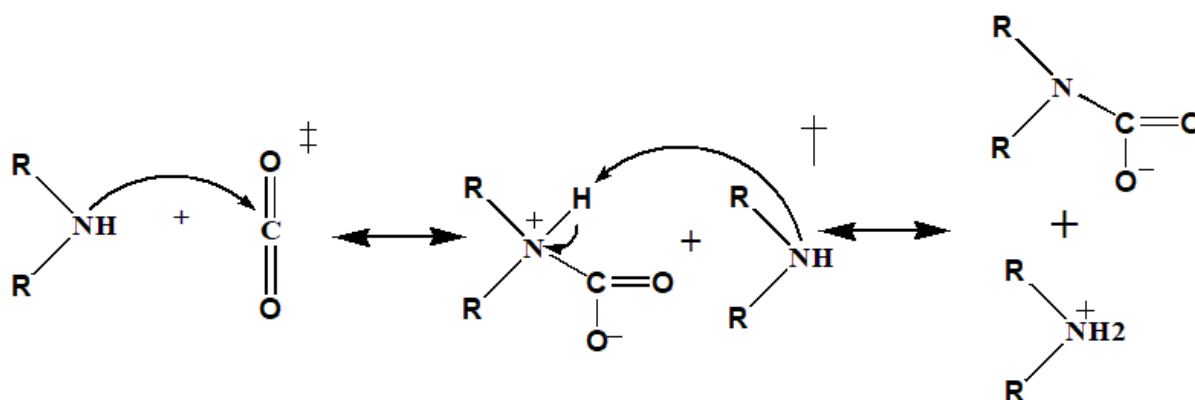


Figure 3: Arrow pushing mechanism between primary amine and $CO_2$ to form a zwitterion (‡), then deprotonate zwitterion to form charged species (†).

Several reported chemisorbents use primary amines to capture $CO_2$ from atmosphere. Among the most successful of these systems, several have achieved capacities on the order of 1 to 5 mmol(g$^{-1}$) [31, 54, 58, 19, 62, 35, 25, 32, 56]. Several reported chemisorption systems attempted to attach amine-rich monomers to fabric substrates given their high surface area and ease of processing [58, 32, 56]. Early work by Li et. al. attempted to functionalize glass fibers using a wet impregnation method, but later work identified the potential for graft polymerization to form more robust sorbents with higher fractions of monomer attachment [31, 32].

Reported approaches by Yang *et. al.* and Wu *et. al.* to functionalize fabric by grafting amine-rich monomers to fabrics used a two-step initiation procedure; monomers were initiated with peroxides and fabrics initiated with ionizing radiation [58, 56]. Initiation

forms free radicals on which monomers polymerize. Both Yang *et. al.* and Wu *et. al.* reported high $CO_2$ capacities, 6.22 and 4.8 mmol$(g^{-1})$ respectively, but synthesized their sorbent through a two-step process that lends itself to undesired homopolymerization of monomer and adds additional cost to potential mass production [58, 56, 17]. This work reports on the fabrication of $CO_2$ sorbents with a novel single step graft polymerization procedure to attach amine-rich monomers to consumer-grade polymeric fabrics. We grafted allylamine and 3-buten-1-amine (butenylamine), shown in figure 4, onto polyethylene terephthalate (PET), high-density polyethylene (HDPE), and Nylon-6 (Nylon) via radiation-induced graft polymerization (RIGP).

## 3.2 Methodology

### 3.2.1 Monomer Selection

A main goal of this study is to develop a single-step synthesis of a commercial-grade atmospheric $CO_2$ sorbent through the use of radiation-induced graft polymerization. Additionally, this study aims to initiate graft polymerization chemically with the use of peroxides and nitroxides. In order to synthesize fabrics with the capability to capture $CO_2$, monomers must be attached onto the backbone of the fabric. Thus, the monomer we select must meet two main criteria: it must be able to attach to our selected fabrics (PET, HDPE, Nylon) and must be capable of capturing $CO_2$ from ambient air. As a result, our selected monomers contain a vinyl group which allows the production of a free radical, providing a site for the monomer to attach onto the substrate. The monomers also contain primary amine groups, allowing for $CO_2$ sequestration. The two monomers initially selected were allylamine and butenylamine, with the bond line structure for each shown in Figure 4 below. Both monomers are toxic as individual molecules. This toxicity emerges as the small monomers have vinyl groups and primary amines that could react with key systems in the body. However, after polymerization and the removal of unreacted monomers, the compounds can no longer be absorbed into the skin and pose no risk of reaction in the body. Additionally, the polymers formed are largely unreactive with the environment and thus unlikely to break off the substrate back into their original

11

form. It is more likely for a non-harmful compound, such as ammonia, to be formed in the case of a reaction atmospheric ozone or another compound because of the lower bond energy of C-N bonds compared to C-C bonds.
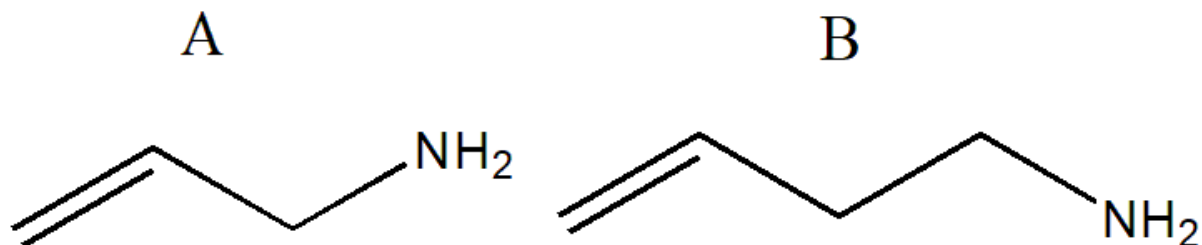


Figure 4: Bond line structure of (A) allylamine and (B) 3-butenylamine.

In this study, the $CO_2$ sorbency of the selected monomers was verified through impregnation of activated carbon with the selected monomers and characterization of $CO_2$ capacity. According to Gholidoust et al., preparation of activated carbon samples is dependent on wet impregnation, a process in which the monomers physically attach to the activated carbon. In accordance with this method, each monomer was dissolved in 20 mL of water to form an aqueous solution [20]. This solution was then poured into a beaker containing 5 g of activated carbon, and stirred for 2 hours at 40 ℃. Next, the samples were dried in a desiccator and massed to determine the degree of attachment (DoA), calculated using the following equation where $m_0$ is the original mass of the activated carbon sample before attachment and $m$ refers to the mass of the sample after impregnation with monomer.

$$\text{DoA} = \frac{m - m_0}{m_0} \times 100 \tag{3}$$

The activated carbon samples produced were then placed in a chamber filled with 100 % $CO_2$ atmosphere. The $CO_2$ concentration was then measured over time to compare the $CO_2$ sorbency of the respective monomer solutions. All $CO_2$ sorbency tests were conducted at atmospheric pressure and 22 ℃ for 30 min each. The results shown in Figure 11 indicate that the impregnation of both allylamine and butenylamine increased the sorbency of the raw activated carbon by a significant amount.

A large portion of the monomer impregnated into the activated carbon was likely bound into the bulk of the material. These amine-containing monomers bound within the bulk are likely to contribute less to the $CO_2$ capacity as opposed to surface amines, as the $CO_2$ can only attach to bulk amines after diffusion into the activated carbon [20]. Due to this phenomenon, the impregnated carbon samples do not effectively model the expected absorbency of our functionalized fabrics. Instead, $CO_2$ absorbance was used as a qualitative measure to both confirm the $CO_2$ sorbency of our fabrics and compare the two monomers. As both impregnated carbon samples showed improved $CO_2$ sorbency as opposed to raw activated carbon, we concluded that both allylamine and butenylamine absorb $CO_2$ from ambient air.

As shown by Figure 11, allylamine exhibits a significantly higher $CO_2$ sorbency as opposed to butenylamine per unit mass of loaded activated carbon. The difference in mass-normalized $CO_2$ sorbency can likely be attributed to the difference in amine density between the two monomers we have selected. The bond line structures in Figure 4 show that allylamine contains one fewer CH2 group than butenylamine, yielding a difference in molar mass of 14.03 g(mol-1). Despite the additional CH2 group on butenylamine, both monomers contain the same number of amine groups per molecule. Consequently, allylamine contains 24.57 % more primary amine groups per gram than butenylamine. Therefore, 1 g of allylamine would theoretically have a greater $CO_2$ capacity than 1 g of butenylamine.

The difference in primary amine density may also have an effect on the kinetics of the $CO_2$ capture reaction depicted in Figure 17. When placed in environments with excess concentrations of $CO_2$, such as our test chamber, the literature predicts that amine-based sorbents follow pseudo-first-order kinetics depending on the concentration of unreacted amines [53]. As allylamine-impregnated carbon is likely to contain a higher concentration of unreacted amine groups with respect to mass, the $CO_2$ capture reaction for allylamine is likely to proceed at a faster rate. Thus, the difference in amine density is likely to create a discrepancy in the kinetics of $CO_2$ capture in addition to overall capacity. As shown from our experiments, when comparing the two monomers, allylamine exhibited

both an improved $CO_2$ capacity and a superior rate of kinetics for the intended reaction.

Unfortunately, after several trials of grafting the two selected monomers, we were able to determine that the use of butenylamine was no longer cost-effective. Therefore, we looked into alternative monomers with amine groups for $CO_2$ extraction and vinyl groups that allow for grafting. The monomer we selected is diallylamine, and the bond line structure is given in Figure 5 below.
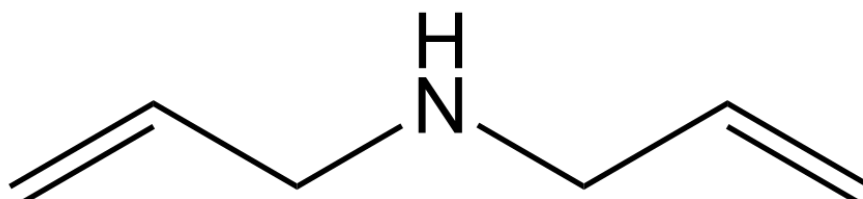


Figure 5: Bond line structure for diallylamine

As opposed to our first two monomer selections, diallylamine contains two vinyl groups which could help to improve the eventual degree of grafting (DoG) of our monomer onto the consumer-grade fabrics. We concluded from our previous activated carbon experiments on allylamine and butenylamine that the amine group on the monomer will abstract $CO_2$ from the atmosphere. Due to this assumption, we concluded that it would not be necessary to conduct $CO_2$ tests on diallylamine-impregnated activated carbon.

### 3.2.2   Radiation Grafting

After validating that the selected monomers do chemisorb $CO_2$ from the atmosphere, we used them to functionalize three commercial-grade fabrics via graft polymerization. This chapter reports the synthesis of graft copolymers between allylamine as well as butenylamine monomers and PET, HDPE or Nylon backbone chains via radiation-induced graft polymerization. Figure 6 displays the mechanism of radiation-induced graft polymerization for each of the three substrate polymers [15, 18, 23, 38, 17]. Incident electron beam radiation causes the abstraction of hydrogen—the ejection of a H from an R'RCH2 group in the backbone polymer—that produces a carbon-centered free radical on the substrate. This carbon-centered free radical attacks the vinyl group of the monomers, forming a

sigma bond and unpaired electron on the newly attached monomer, as indicated in the first propagation step. Monomers continue to add to the growing grafted polymer chain through this mechanism, continuing propagation.
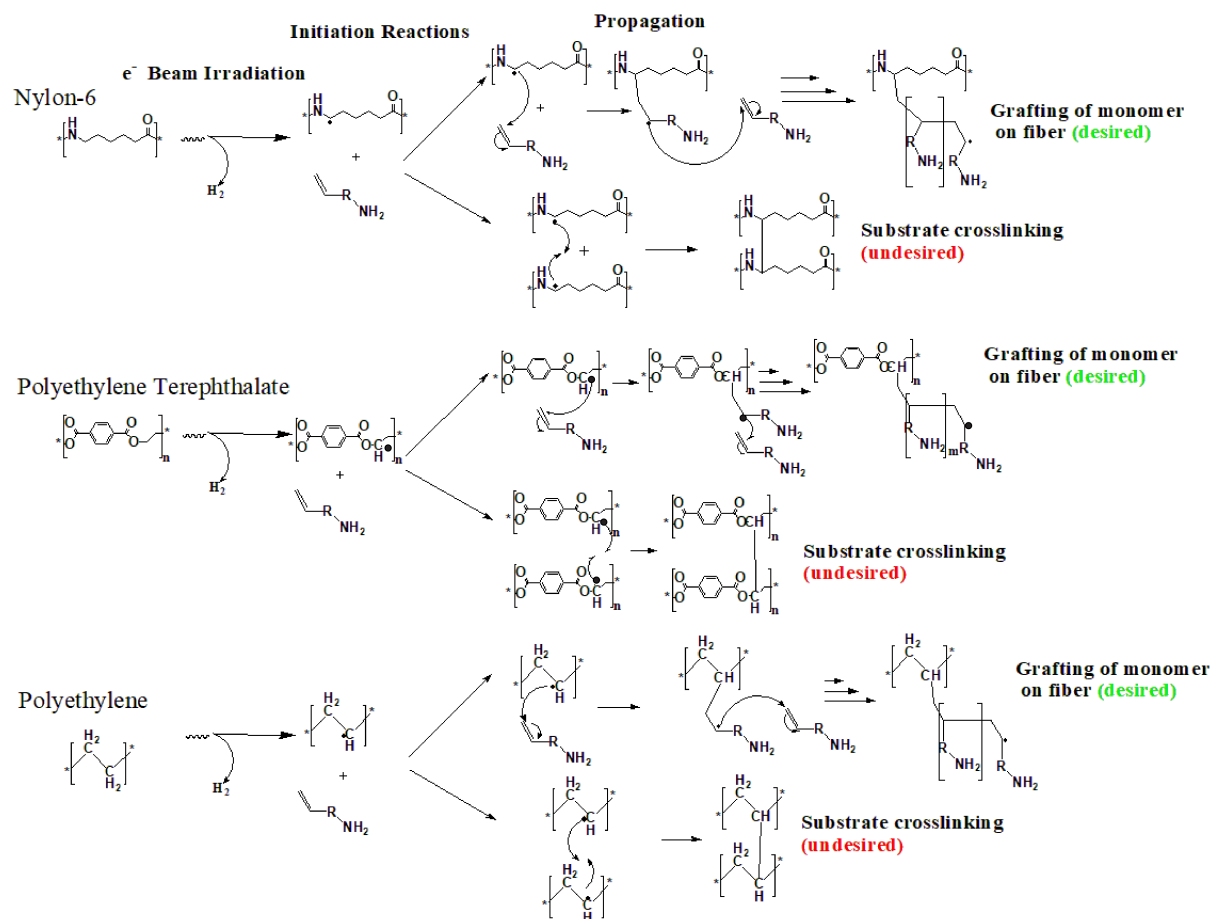


Figure 6: Mechanism of radiation-induced graft polymerization (RIGP), including desired grafting and undesired crosslinking [17]

Before any radiation grafting, the three fabrics were cut into 50-mg square swatches. To synthesize our novel co-polymers, we needed to remove the protective polylactic acid (PLA) coating the manufacturer applied to the PET and HDPE. Refluxing both PET and HDPE in tetrahydrofuran (THF) at a ratio of 20 mL of THF per 50 mg of sample for 4 hours at 70 ℃ removed the PLA coating [17]. After refluxing the PET and HDPE, all three fabrics were washed in methanol and deionized water to remove organic contaminants. We expect that atmospheric organic particulates could react with carbon-centered free radicals to inhibit grafting. After drying, the fabrics were stored and irradiated in 12-mL scintering vials purged with argon.

This work reports the first single-step synthesis of fabric $CO_2$ sorbents via radiation-induced graft copolymerization. The procedure used to irradiate fabrics and grow a graft copolymer via chain polymerization, in Figure 7, follows work reported by Yang *et. al.*, Wu *et. al.*, and Dietz *et. al.* [58, 56, 13, 17].
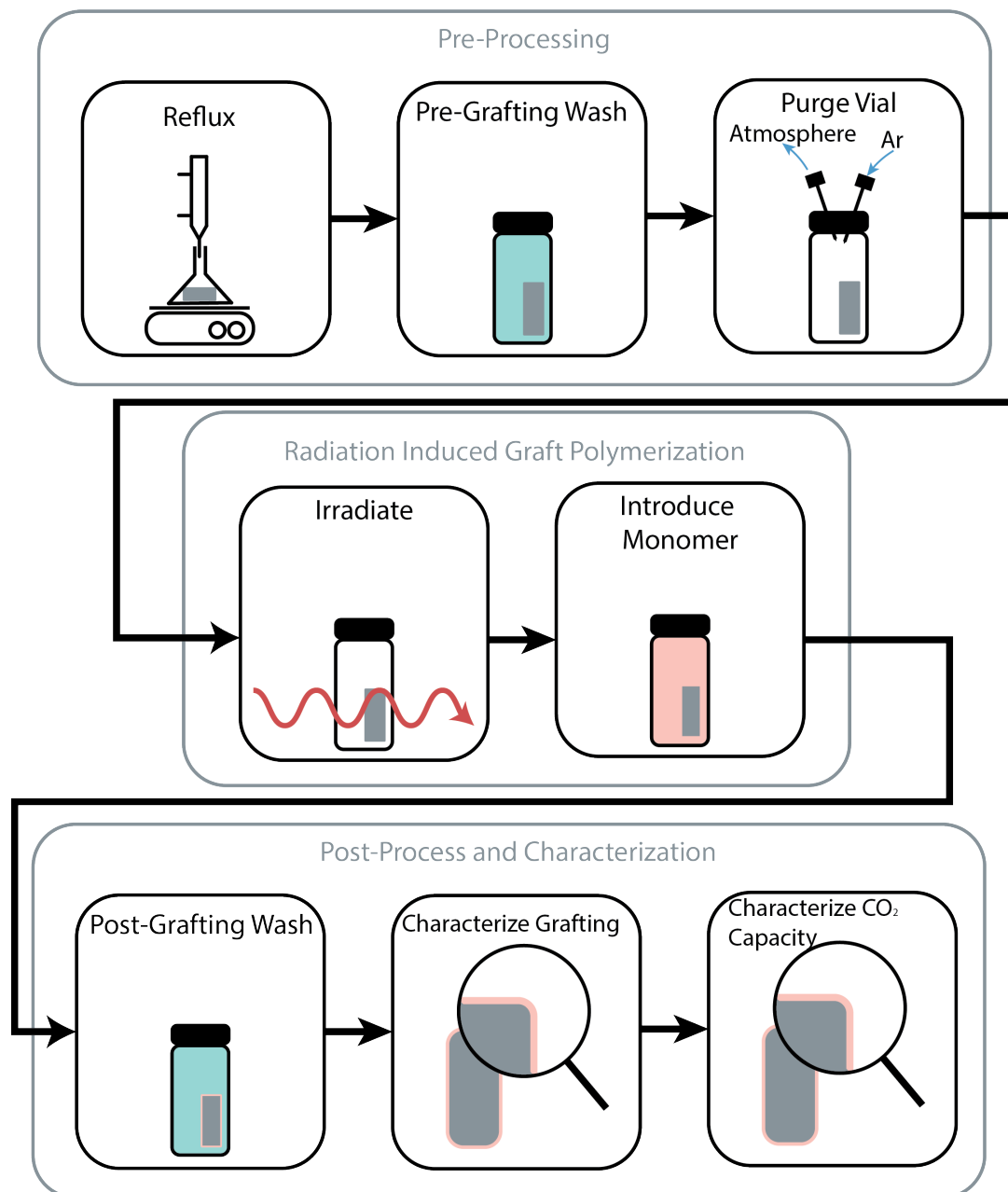


Figure 7: Schematic of process used in synthesizing and characterizing novel graft copolymeric $CO_2$ sorbents

We accessed the Medical Industrial Radiation Facility (MIRF) at the National Institute of Standards and Technology (NIST; Gaithersburg, MD) to perform electron beam irradiation. Dosimetry was performed by correlating the radicals produced in alanine foil

to the counts on a Faraday cup behind the sample stage [13, 12, 17]. A linear correlation between counts on the Faraday cup and dose allowed for the precise tuning of ionizing radiation incident on the fabrics. Fabrics—consisting of individual fabrics stored in vials with an inert Argon atmosphere—were irradiated to either 150 kGy or 250 kGy at an energy of approximately 10.5 MeV to generate approximately $10^{17}$ to $10^{19}$ free radicals per gram in PET, HDPE and Nylon [15]. During irradiation, fabrics were kept in a heat insulated container with dry ice and rotated through the beam path on a turntable, as depicted in figure 8.
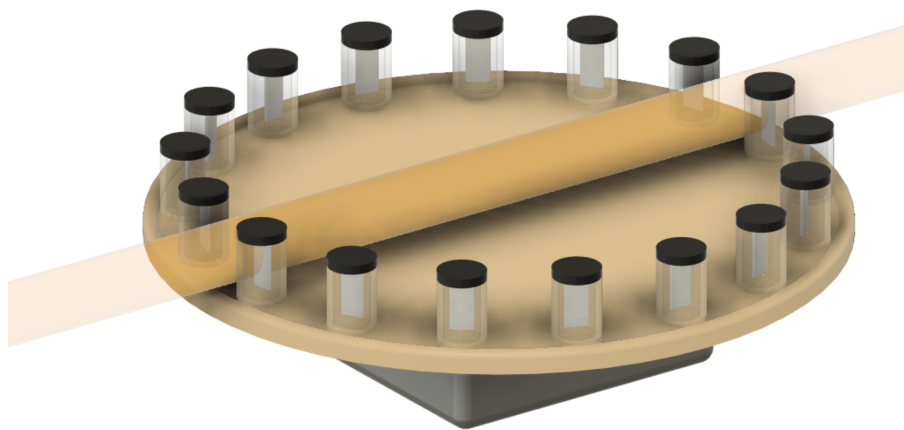


Figure 8: Rendering of turntable used to cycle fabric samples, depicted as white rectangles in clear vials, through the electron beam path, depicted as the translucent yellow line.

The cryogenic temperatures reduce the rate of radical recombination, increasing the fraction of radicals available to react with monomer [13, 17]. These conditions contribute to an increase in monomer attachment. After irradiation, approximately 10 mL of monomer was introduced to each vial containing the substrate fabrics. Upon introduction of the monomer, free-radical chain graft copolymerization proceeded as depicted in figure 6.

After grafting, the fabrics were washed to remove any homopolymerization. Washing consisted of rinsing, vortexing, then sonicating samples in aqueous and organic solvents—specifically water and methanol. Sample fabrics were then dried in a vacuum desiccator to remove all solvents while avoiding unintended $CO_2$ sorbency that could interfere with

later characterization.

### 3.2.3 Characterization by Fourier Transformation Infrared Spectroscopy

In a Fourier Transform Infrared (FTIR) Spectrometer, functional groups in a sample are measured by the wavelength of light they absorb for vibrational transitions [26]. FTIR measures the interference between a split beam of IR light covering a wide range of wavelengths; one beam passes through the sample and interferes with the one that does not. This produces an interference pattern that yields a spectra of absorption as a function of wavenumber when subject to Fourier analysis. This absorption spectra reveals the functional groups in the sample; each peak corresponds to a characteristic vibrational transition for each group.

Fourier-Transform infrared attenuated total reflectance (FTIR-ATR) spectrum was recorded with the Thermo Fisher Scientific (Waltham, MA) Nicolete iS-50 FTIR with a Smarte iTX diamond window ATR module. In ATR mode, the beam is reflected rather than transmitted through the sample. Measurements consisted of an average of 120 scans performed at a resolution of 2 cm$^{-1}$. Growth in peaks at 764, 1,619, 3,360 and 3,442 cm$^{-1}$ that correspond to NH wag, bend, symmetric and asymmetric stretch, respectively, along with 1,261 cm-1 for CN stretch confirm monomer attachment [17, 26].

### 3.2.4 Characterization by Scanning Electron Microscope and Energy Dispersive Spectroscopy

The morphology and elemental composition of the fabric samples after both grafting and $CO_2$ adsorption testing were determined with scanning electron microscopy (SEM) along with an energy dispersive spectroscopy (EDX) analyzer. The Hitachi S-3400 Variable Pressure SEM (Tokyo, Japan) was used to collect the data. SEM images and EDX spectra were obtained from three unique physical locations on each fabric sample under variable pressure mode at 100 Pa. Additionally, elemental compositional data obtained from linescans were analyzed and compared. All measurement processes used an accelerating voltage of 15 kV, and the magnification used for each image remained in the range of

375X to 475X.

### 3.2.5 CO$_2$ Capacity Characterization

CO$_2$ capacity, typically measured in mmol of CO$_2$ captured normalized by mass or moles of sorbent, comprises the figure of merit for CO$_2$ sorbent devices [38, 17]. Characterizing CO$_2$ capacity typically requires exposing the sorbent to an atmosphere with a well controlled CO$_2$ concentration and measuring its decrease. Our work followed the methodology established by Ho *et. al.*, where an airtight chamber was filled with a known CO$_2$/Ar gas mixture and measured the drop in concentration of the former using an IR sensor [22, 17]. To better resolve drop in CO$_2$ concentration, this study included the design, fabrication, and use of two chambers—one for fabrics and one for activated carbon. As indicated in Figure 3, the amount of monomer directly impacts the amount of CO$_2$ adsorbed. Thus, we expected the fabric samples to adsorb far less CO$_2$ given the smaller total amount of monomer attached per sample as compared to activated carbon [17]. To properly resolve the smaller expected CO$_2$ adsorption from fabrics, we designed a smaller chamber. Figure 9 shows a render of both chambers and a schematic of their functional components.
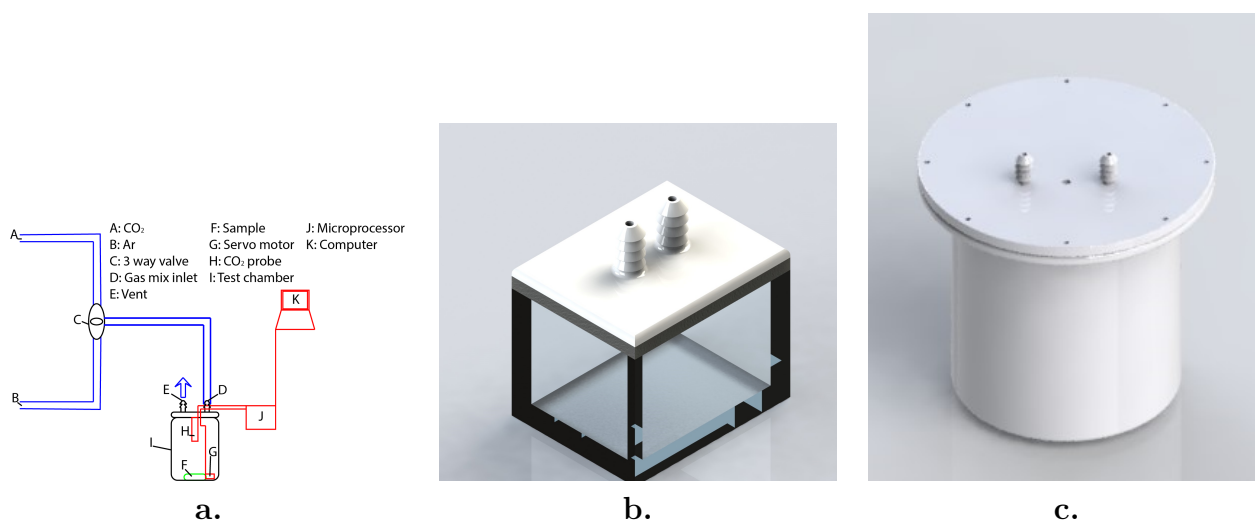


Figure 9: A generalized schematic for the (a) test chamber and a (b) detailed rendering of the test chamber for fabric samples and (c) activated carbon samples [17]

    Both the cylinder and lid of the chamber designated for testing activated carbon samples were manufactured via fused filament fabrication additive manufacturing. We

fabricated the box of the chamber designed for fabric samples with laser-cut acrylic joined with acrylic cement and sealed with silicon rubber sealant.

Both chambers used a CozIR infrared sensor to measure the concentration of $CO_2$ in atmosphere through the absorbance of characteristic IR frequencies. A metal filament heated through joule heating generates a range of IR frequencies. A detector at the opposite end of the sensor records absorbance of characteristic wavelength bands associated with $CO_2$: 2.7 $\mu$m, 4.3 $\mu$m, and 15 $\mu$m. To confirm that the chamber and sensor accurately measure $CO_2$ concentration in the chamber, we created a calibration curve to correlate the measured $CO_2$ fraction with a carefully controlled input $CO_2$/Ar ratio. We manipulated the input gas mix with the use of two flowmeters. Figure 10 indicates that the measured $CO_2$ concentration closely matches the input $CO_2$ fraction. This calibration curve also supports that both fabric and activated carbon tests were performed within the proportional region of the detector.
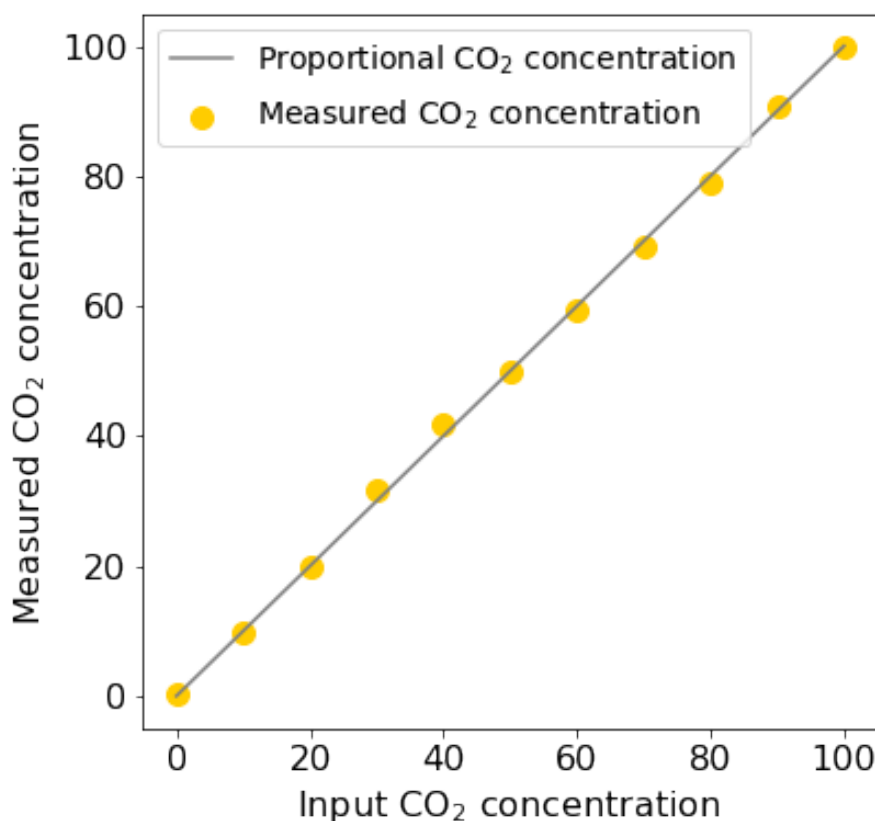


Figure 10: Calibration curve of input $CO_2$ concentration and measurements identified by CozIR sensor [17]

Before measuring the capacity of AC or fabric sorbents, we first collected a background decay in $CO_2$ concentration, which likely stemmed from a leak in the chamber. Since neither chamber was prepared under clean room conditions, contaminants likely prevented a perfectly airtight seal [43]. Once ready to measure, the sample was inserted, and the servo was actuated to lower a lid over the sample. This protected the sample from unintended $CO_2$ adsorption before measurements were taken. We then flooded the chamber with a known $CO_2/Ar$ ratio. Once the atmosphere in the chamber stabilized at the desired $CO_2$ concentration the servo was actuated to expose the sample. The CozIR sensor measured $CO_2$ concentration as a function of time, and equation 4 enabled the identification of $CO_2$ capacity.

$$capacity(mmol(g^{-1})) = 10^{-6}\Delta[CO_2]nV(\frac{n\rho_{CO_2}}{m_{CO_2}} + \frac{(1-n)\rho_{Ar}}{m_{Ar}})M^{-1} \qquad (4)$$

## 3.3  Results and Discussion

### 3.3.1  Confirmation of Monomer $CO_2$ Capacity

Following the procedures for wet impregnation of activated carbon from Ho et al. and the degree of attachment (DoA) measurements determined by equation 3, the attachment of allylamine and butenylamine on activated carbon was quantified in Table 1.

Table 1: Degree of Attachment for the wet impregnation of both monomers [17]

| Monomer | Degree of Attachment | Standard Error |
|---|---|---|
| Allylamine | 73.12 | 7.05 |
| Butenylamine | 71.11 | 11.48 |

Samples were prepared by mixing the monomer and activated carbon in a 0.8 ratio by weight, resulting in a theoretical DoA of 80 %. The discrepancy between experimental and theoretical DoA likely stemmed from the preparation procedure. The attachment occurs while the carbon is in a slurry; thus, the transfer of the mixture between containers during sampling leaves behind small amounts of residue.

The $CO_2$ capacities of both unloaded and monomer-impregnated activated carbon can be found in Figure 6. All $CO_2$ sorbency tests were conducted at atmospheric pressure

and 22 °C for 30 minutes, and the error bars result from standard error calculations from six samples for each attachment configuration. As evident in figure 11, impregnated activated carbon outperformed unloaded activated carbon in terms of $CO_2$ capacity by a significant amount.
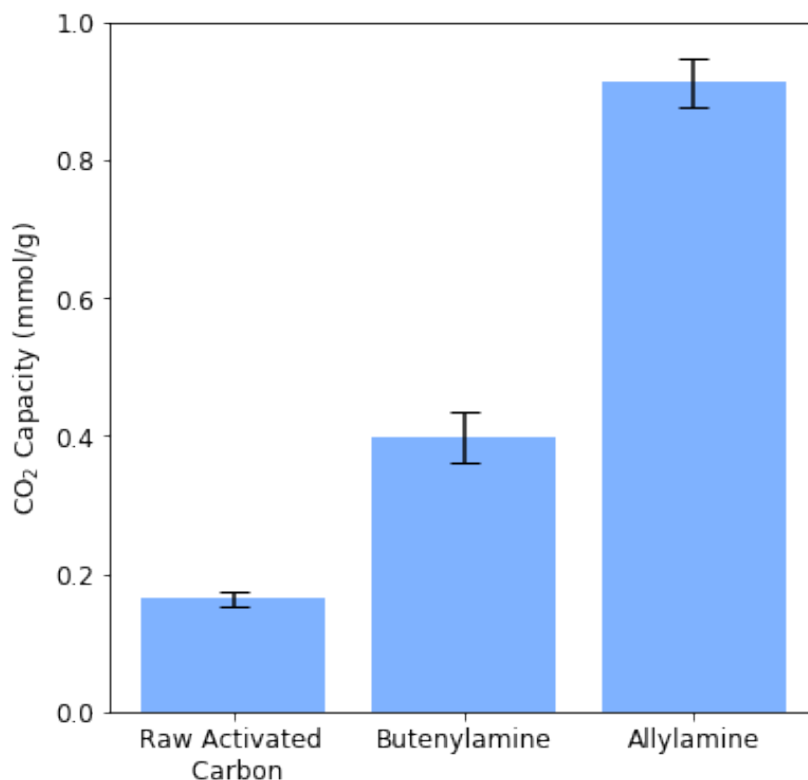


Figure 11: Adsorbance capacity of raw and monomer impregnated activated carbon [17]

Much of the monomer impregnated into the activated carbon was likely bound into the bulk of the material, reducing the overall capacity of the absorbent. Because bulk amines could only absorb $CO_2$ following diffusion through the activated carbon, they contributed to $CO_2$ capacity less than surface amines did [20]. As a result, the results from activated carbon testing can only be used to compare capacity qualitatively and does not accurately approximate the expected absorbances of functionalized fabrics.

Activated carbon samples impregnated with either monomer exhibited higher capacity than the unprocessed material; therefore allylamine and butenylamine successfully chemisorb $CO_2$. Due to its significantly higher $CO_2$ capacity on activated carbon, allylamine exhibited better mass-normalized sorbency properties than butenylamine. The

disparity between the two monomers can be attributed to the likely higher amine density with allylamine. Allylamine has a lower molar mass than butenylamine by 14.03 g(mol$^{-1}$). Because of this difference in molar mass, allylamine contains 24.57 % more primary amine groups per gram than butenylamine, resulting in a greater $CO_2$ capacity per gram.

The higher primary amine density in allylamine may also result in faster kinetics of the $CO_2$ capture reaction. In excess concentrations of $CO_2$, literature dictates that amine-based sorbents follow pseudo-first order or second order kinetics depending on the unreacted amine concentration [53]. Within the thirty minutes allotted for capacity measurements, more monomers of allylamine reacted to absorb $CO_2$. It can be concluded that allylamine exhibited greater $CO_2$ capacity than butenylamine and a non-loaded standard because of its greater amine density and faster kinetics of absorption.

### 3.3.2 Monomer Attachment

After grafting allylamine and butenylamine onto the selected fabrics, we used three methods to confirm the formation of a graft copolymer composed of clean fibers and amine-rich monomers: 1. gravimetric analysis; 2. Fourier-transform infrared (FTIR) spectroscopy; and 3. energy dispersive spectroscopy (EDX). This study also employs the use of scanning electron microscopy (SEM) in order to assess morphological changes to the fibers. This study implements gravimetric analysis in order to confirm that our clean fabrics exhibit an increase in weight upon grafting. Assuming that no mass is gained or lost due to irradiation, any mass change can be attributed to the addition of nitrogenous monomers onto the fabric. This mass change is reported via degree of grafting (DoG), calculated using equation 5.

$$\text{DoG} = \frac{m - m_0}{m_0} \times 100 \tag{5}$$

It is essential to thoroughly clean the fabrics to ensure that any increase of mass is due to the grafting of monomer onto the backbone, rather than the formation of homopolymer physically attached to the substrate. After three cycles of washing and desiccation, the

23

DoG values for all six polymers were calculated and are shown in Figure 12 below.
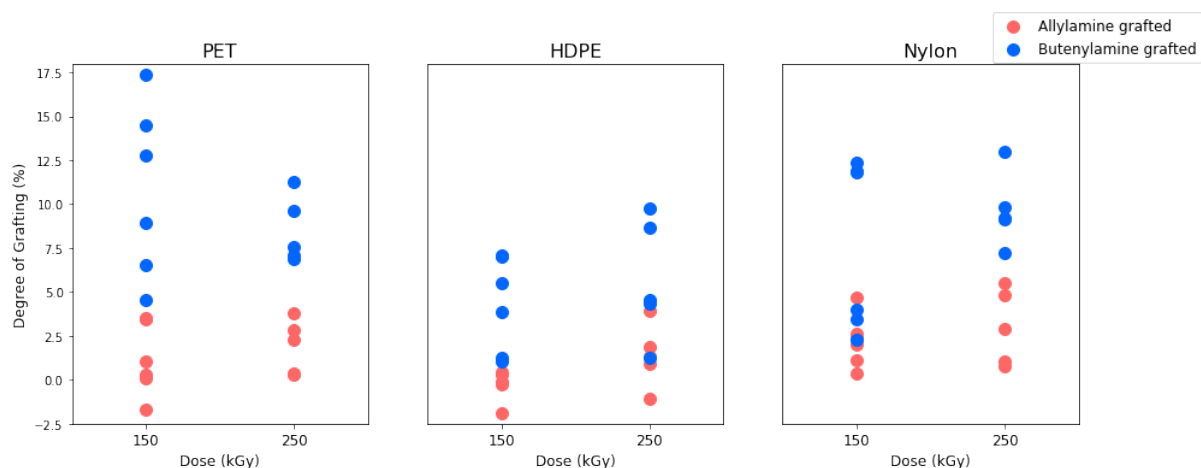


Figure 12: Degree of grafting of allylamine (red) and butenylamine (blue) as a function of dose for all three fabrics [17].

As shown in the figure, fabrics grafted with butenylamine exhibited a greater monomer attachment than those grafted with allylamine. This disparity in degree of grafting can likely be attributed to the different structures of our two monomers. Butenylamine contains one extra CH2 group on the chain. Therefore, the butenylamine has an additional carbon on the backbone separating the amine and the vinyl group. As indicated by the aforementioned free-radical mechanisms, the graft copolymerization step requires reactions between free radicals generated on the vinyl group and the $\pi$-bond of another monomer. Thus, we can conclude that the rate of copolymerization is determined by the reactivity of the free radical generated by radiation. Unfortunately, the presence of amine groups have been shown to stabilize and subsequently eliminate free radicals [55]. This phenomenon may be responsible for the difference in DoG values, as the amine group on allylamine is one carbon closer to the vinyl group when compared to butenylamine. Additionally, as expressed previously, allylamine exhibits a greater amine density when compared to butenylamine. When combining these effects, the allylamine-centered radicals are less reactive, which may explain the difference in grafting between the two monomers.

In addition to gravimetric analysis, this study also employs the use of FTIR to confirm the presence of specific chemical bonds following the grafting procedure. Specifi-

cally, we aim to identify the growth of certain peaks associated with bonds present on our monomers. Each of our two monomers will only possess one functional group once grafted to the substrate: primary amines bonded to an sp3 hybridized carbon. On an FTIR spectra, primary amines exhibit peaks at 764, 1619, 3360, and 3442 $cm^{-1}$, corresponding to the vibrational modes of NH wag, bend, symmetric and asymmetric stretch, respectively [8]. Additionally, successful monomer attachment is indicated by the presence of a peak at 1261 $cm^{-1}$, which corresponds to the CN stretch [27]. Upon comparison between un-grafted and grafted fabrics, we can confirm attachment of the nitrogenous monomer with the identification of the peaks given above. Figure 13 below shows examples of three sample spectra for each fabric.
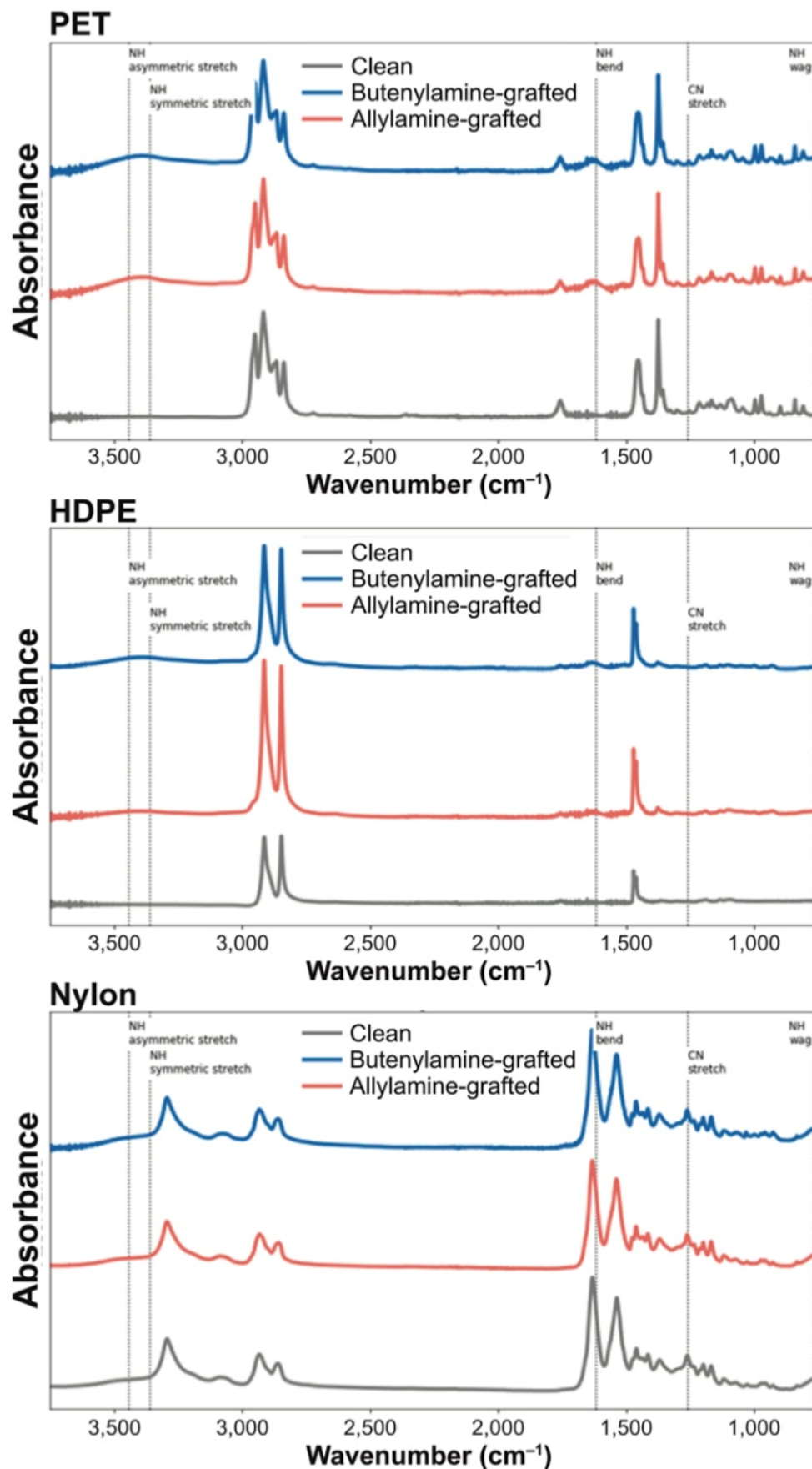
Figure 13: FTIR spectra of HDPE, PET, and Nylon highlighting the growth in the peaks associated with primary amines [17]

As shown by the figure, both PET and HDPE exhibit small growth in peaks for the NH stretching mode when grafted with allylamine and butenylamine. These small peaks at 3442 cm$^{-1}$ and 3360 cm$^{-1}$ combine to form one broad peak centered between the two values above. Unlike PET and HDPE, however, Nylon does contain an amine group. Because the grafted monomers make up a very small fraction of the final Nylon-monomer copolymer, the growth of the NH stretch and wag peaks due to monomer attachment is concealed by the characteristic peaks of Nylon. The signal from Nylon's secondary amine also conceals the growth of the CN stretch peak. The CN stretch corresponds to the location of a CO stretch in PET [28, 34]. The signal from the CO group in PET may overwhelm the peak growth at 1261 cm$^{-1}$ due to monomer attachment, explaining the lack of increased intensity shown by PET samples. Given the growth of both NH stretch peaks at 3442 cm$^{-1}$ and 3360 cm$^{-1}$ in all samples and NH bend and wag at 1619 cm$^{-1}$ and 764 cm$^{-1}$ in PET and HDPE, we can qualitatively confirm monomer attachment. Table 2 below highlights the DoG values of the fabrics used to produce the spectra highlighted in Figure 13.

Table 2: Degree of Grafting for the fabrics with FITR spectra displayed in figure 13

| Fabric | DoG Butenylamine grafted | DoG Allylamine grafted |
|--------|--------------------------|------------------------|
| PET    | 17.36                    | 3.76                   |
| HDPE   | 7.05                     | 4.85                   |
| Nylon  | 11.85                    | 2.30                   |

Finally, EDX was implemented to confirm the success of grafting through elemental analysis. Specifically, we look to use EDX to confirm the increase in the nitrogen content present in our fabrics, due to the addition of nitrogen-rich monomers. Figure 14 below provides a comparison between the nitrogen content present in the clean fibers and the grafted fabrics.
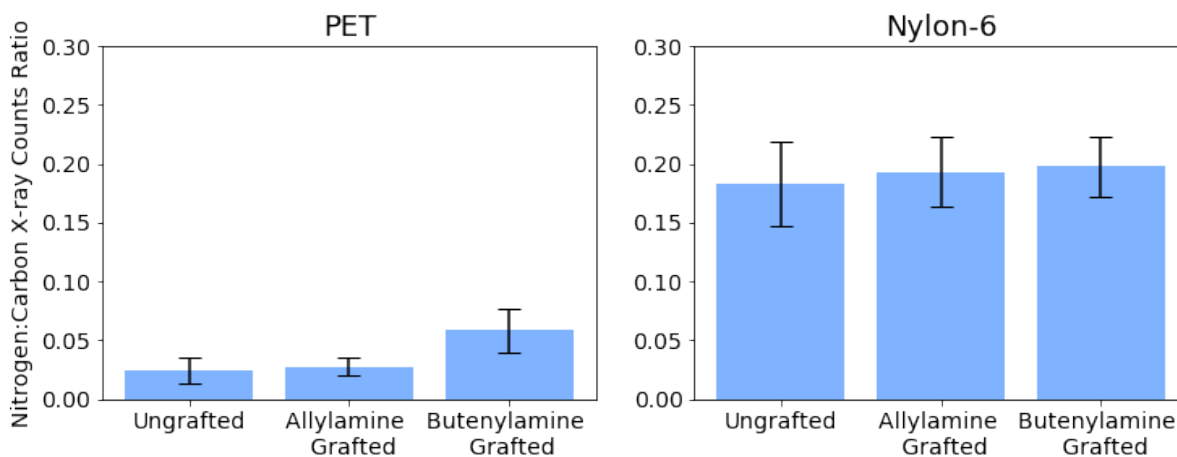
Figure 14: Nitrogen to carbon ratios obtained from EDS for both PET and Nylon fabrics generated with allylamine and butenylamine compared to ungrafted samples [17]

As shown in the figure above, each grafted sample exhibited a greater nitrogen content with respect to each ungrafted fabric. The error bars shown represent the standard deviation between the nitrogen concentration recorded at three different points across the fabrics. Although EDX provides us with raw values, the comparison of elemental concentration between grafted samples is primarily used as a qualitative measure of the success of the grafting process. Thus, we can use Figure 14 to qualitatively confirm the attachment of our nitrogenous monomers onto the various fabrics. Qualitatively, the growth in nitrogen content of HDPE was much lower than the growth shown in PET and Nylon samples. This is likely due to the fact that the volume and texture of the HDPE fibers was such that only a small percentage of the interaction volume of the electrons used in EDX overlapped with the bulk fiber. This produced a spectra with a very low signal-to-noise ratio, thus the EDX results for HDPE samples were not reported.

Additionally, the EDX mapping feature allows for a direct view of the dispersion of the amine-rich monomer; an example is provided in Figure 15 below. The figure clearly shows the presence of nitrogen in the fabric. As raw PET does not contain any nitrogen, we can conclude that the presence of nitrogen confirms the attachment of our monomers.
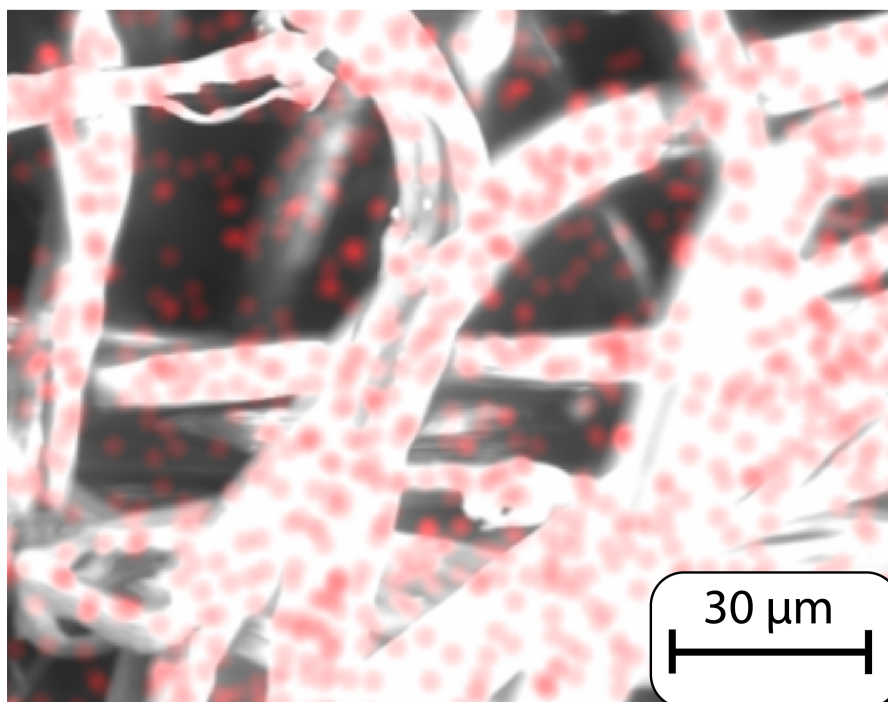
Figure 15: EDS map of PET grafted with butenylamine, DoG of 14.48 %. Observed nitrogen is colored red and the secondary electron image is colored red [17]

Finally, SEM was used to evaluate the morphological changes to the fibers due to radiation and the introduction of our monomer. An image of PET fibers before and after grafting is given in Figure 16 below.
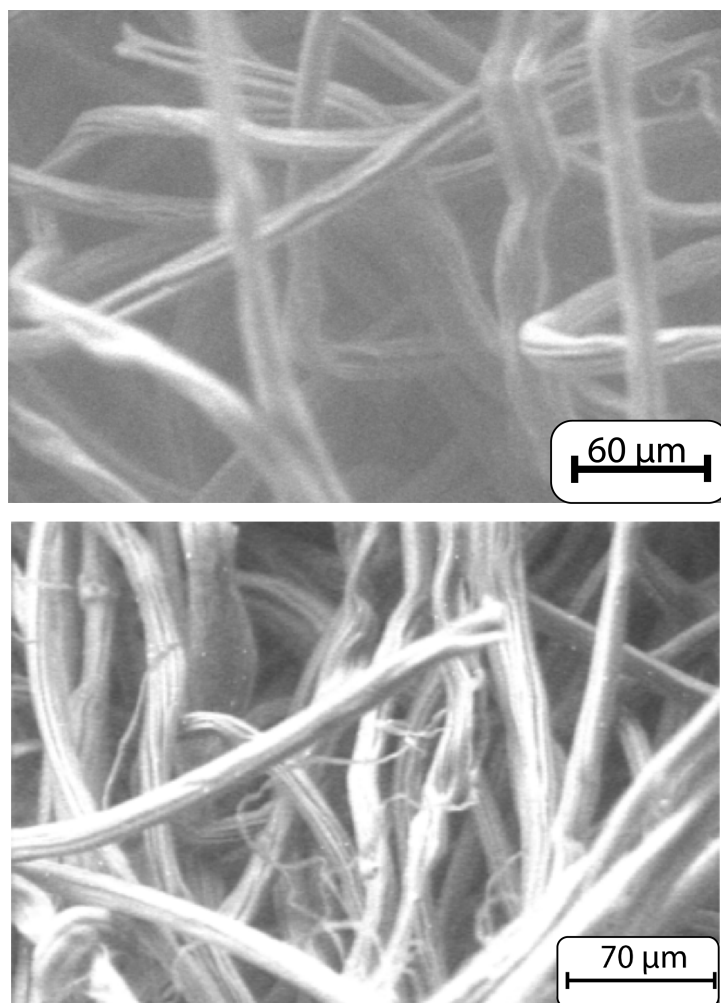
Figure 16: PET fibers before (A) and after (B) grafting of allylamine monomer at 150 kGy. No significant structural damage or homopolymer buildup was observed after radiation [17]

The figure shows that the fibers composing the fabrics maintained similar physical characteristics following the grafting procedure. Additionally, there was little to no buildup of homopolymerized allylamine or butenylamine on the surface of the fibers, ensuring that any monomer present is indeed covalently bonded to the backbone of the substrate. The figure also indicates that the grafting was not localized, but instead grew uniformly along the polymer backbone. The absence of visible localized polymerization can indicate a low probability of propagation along grafted chains. Rather, the reaction favors the grafting of small chains attaching to the backbone. Figure 16 also shows the minimal amount of degradation due to radiation, as the grafted fabric looks morphologically similar to the raw fabric. The polymers that are used as a substrate for grafting

primarily undergo crosslinking as a result of ionizing radiation; however, it is expected that limited aging via chain degradation may have occurred [15, 3].

### 3.3.3 $CO_2$ Capacity, Kinetics, and Mechanisms

Figure 17 depicts a characteristic decay curve of $CO_2$ concentration as a function of time when exposed to a PET-allylamine copolymer. As indicated in figure 3, the reaction between $CO_2$ and primary amines reported in this study depends on both the concentration of primary amines and atmospheric $CO_2$. Thus, the reaction theoretically matches second-order kinetics. Given that the method of characterizing $CO_2$ adsorption produces time-dependent decay curves, this study includes analysis of the reaction kinetics between our novel sorbents and $CO_2$. The $CO_2$ concentration decay over time was used to confirm second order kinetic behavior and identify the rate constants or adsorption for each copolymer.
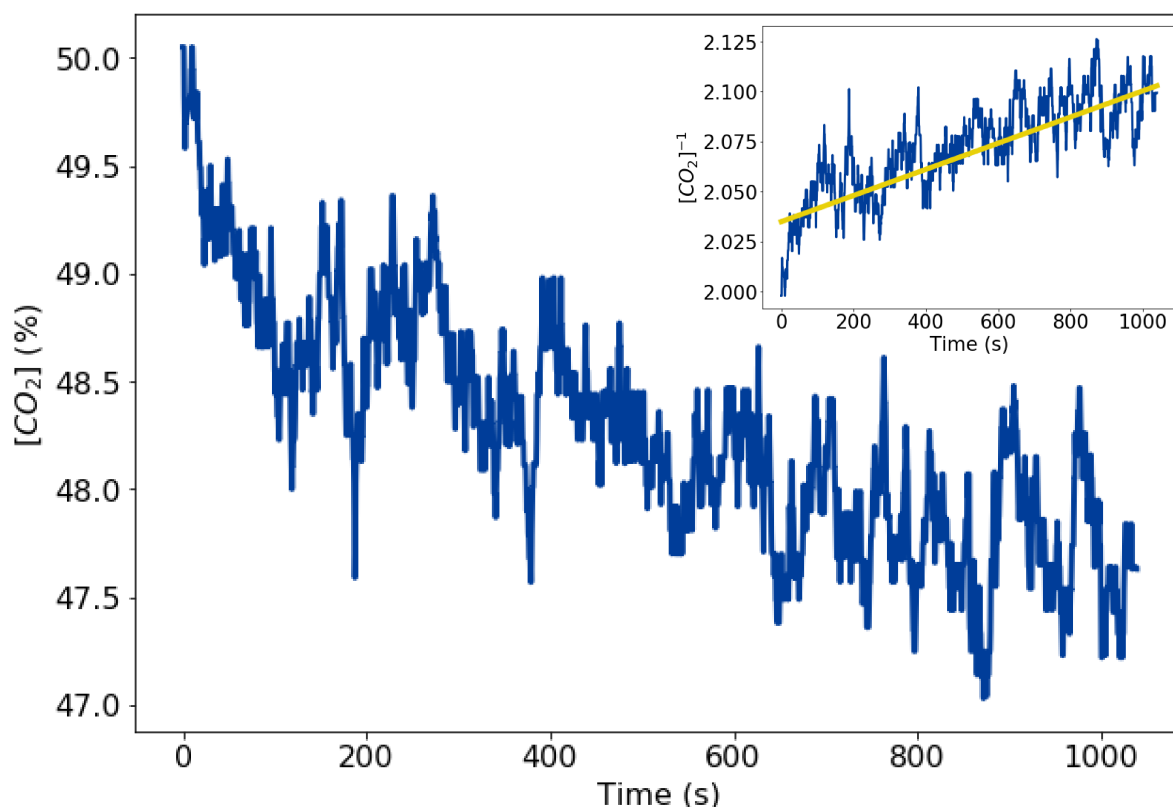


Figure 17: A characteristic decay in $CO_2$ concentration from adsorption on allylamine-grafted PET as a function of time. The insert displays a second order kinetics fit with an effective rate constant of 6.54 x 10-5 $(M(s))^{-1}$ [17]

31

The decay curve of $CO_2$ in atmosphere in the presence of fabric depicted in figure 17 was used to identify the rate constants for the reaction between the sorbents and $CO_2$. As indicated by a comparison of R2 values between first and second-order kinetic models, the latter better describes the $CO_2$ sorbent reaction [17]. This contradicts previous findings of pseudo-first order kinetic behavior [53]. Table 3 gives the second order kinetic rate constants for each copolymer. Given the similar rate constants between each copolymer, the kinetic behavior of the material system described in this study does not depend significantly on the fabric or monomer.

Table 3: Rate constants for second order kinetic behavior for $CO_2$ sorbency [17]

|  |  | $k_{eff}$ $(mole(s))^{-1}$ | Standard deviation $(mole(s))^{-1}$ | n |
|---|---|---|---|---|
| PET | Allylamine | $4.61 \times 10^{-5}$ | $1.96 \times 10^{-5}$ | 8 |
|  | Butenylamine | $3.04 \times 10^{-5}$ | $1.42 \times 10^{-5}$ | 10 |
| HDPE | Allylamine | $3.83 \times 10^{-5}$ | $2.13 \times 10^{-5}$ | 10 |
|  | Butenylamine | $4.51 \times 10^{-5}$ | $3.21 \times 10^{-5}$ | 9 |
| Nylon | Allylamine | $5.11 \times 10^{-5}$ | $4.62 \times 10^{-5}$ | 9 |
|  | Butenylamine | $4.27 \times 10^{-5}$ | $2.09 \times 10^{-5}$ | 5 |

Figure 18 displays the $CO_2$ capacities of each novel copolymer synthesized via RIGP: PET, HDPE, and Nylon grafted with allylamine and butenylamine. The error bars in the figure represent a 2.5 % uncertainty per recommendation by CozIR—e.g. error bars of $\pm1.25$ % for a raw concentration of 50 %. These error bars are treated as shot noise and give the noise floor of the $CO_2$ concentration measurements. Any fabric where the error bars do not capture the 0 mmol$(g^{-1})$ value exhibited statistically significant absorbance. All $CO_2$ sorbency tests were performed in a well controlled atmosphere of 50 % $CO_2$ and 50 % Ar at 22 °C, per the procedure described in 3.2.5.

Figure 18.a. presents $CO_2$ sorbency in units of mmol of $CO_2$ absorbed normalized by the mass of each sorbent, including both fabric and grafted monomer. This is the most common figure of merit for $CO_2$ sorbency and enables comparison between sorbents reported in this study and prior work reported in literature [48, 60, 61]. Figure 18.b. presents $CO_2$ sorbency in units of mmol of $CO_2$ absorbed per mmol of monomer attached. This measure allows for an evaluation of the extent of reaction between pri-

mary amines in the grafted monomer and $CO_2$. Given that the $CO_2$ sorbency reaction presented in Figure 3 predicts a $mmol(mmol)^{-1}$ capacity of exactly 0.5, these values allow for an evaluation of the fraction of monomers that react to absorb $CO_2$.

All copolymers with a DoG of higher than 4 % achieved statistically significant $CO_2$ capacity, indicating that they do behave as $CO_2$ sorbents. This study is the first to report the successful fabrication of $CO_2$ sorbents through single-step radiation-induced graft polymerization. Table 4 further confirms that the single step RIGP produced $CO_2$ sorbents; all untreated fabrics did not adsorb $CO_2$ with statistical significance, but the grafted fabrics did.

Table 4: $CO_2$ capacities of untreated fabrics and fabrics functionalized via RIGP; the former did not exhibit statistically significant capacity while the latter does [17]

|  |  | DoG (%) | $CO_2$ capacity $mmol(g^{-1})$ | Instrumental Error $mmol(g^{-1})$ |
|---|---|---|---|---|
|  | Untreated |  | $5.1 \times 10^{-5}$ | .00025 |
| PET | Allylamine | 3.516 | .00044 | .00033 |
|  | Butenylamine | 14.487 | .0012 | .00031 |
|  | Untreated |  | .00014 | .00061 |
| HDPE | Allylamine | 3.920 | .0013 | .00085 |
|  | Butenylamine | 7.058 | .0014 | .00085 |
|  | Untreated |  | .00014 | .00031 |
| Nylon | Allylamine | 4.848 | .00053 | .00032 |
|  | Butenylamine | 12.390 | .00076 | .00028 |
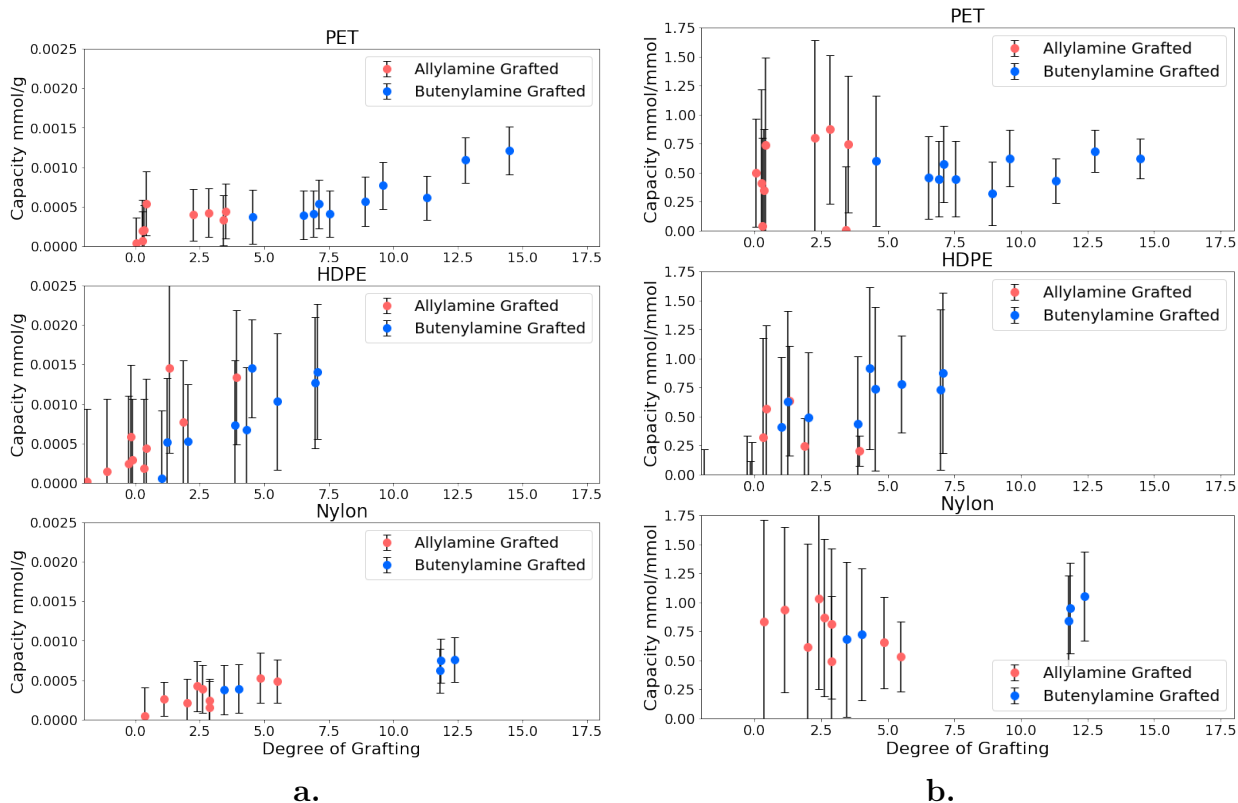
Figure 18: $CO_2$ sorbent capacity reported in mmol($g^{-1}$) (a) and mmol(mmol$^{-1}$) (b) [17]

As indicated in figure 18, the copolymers synthesized via the novel single-step RIGP method investigated in this study achieved statistically significant $CO_2$ sorbency. This result quantitatively validates the single-step RIGP synthesis as a successful means of fabricating $CO_2$ sorbents. As indicated in figure 18, $CO_2$ capacity increases as a function of degree of attachment, similar to $CO_2$ sorbents reported in literature [58, 56]. Thus, enhancing monomer attachment would increase $CO_2$ capacity, potentially to a value comparable to those reported in literature.

Figure 18.b. reports capacity in mmol(mmol$^{-1}$), a measure useful for identifying the extent of amine-$CO_2$ sorbent reaction. Interestingly, the capacity in mmol(mmol$^{-1}$) suggests the presence of alternate mechanisms of sorbency as some of the highest grafted fabrics achieve a capacity higher than 0.5 mmol(mmol$^{-1}$), the theoretical maximum for amine-based chemisorption. One potential mechanism for $CO_2$ extraction may stem from the formation of charged groups from chemisorption, as indicated in figure 3. These charged groups may contribute to physisorption of $CO_2$ given their propensity for strong intermolecular interactions with $CO_2$ molecules with charge separation between oxygen

and carbon atoms. The potential for physisorption is purely speculative based on our understanding of the dominant chemisorption reaction. Though further work is required to confirm physisorption, figure 18.b clearly evidences mechanisms other than posited in figure 3.

# 4 Comparison of Novel $CO_2$ Graft Copolymer Synthesis by Radiation and Chemical Initiated Graft Polymerization

## 4.1 Introduction to Chemical-Induced Graft Polymerization (CIGP)

Prior research by both Yang et. al. and Wu et. al. reported high $CO_2$ capacities—6.22 and 4.8 mmol(g$^{-1}$) respectively—through a two-step synthesis process involving both chemical and radiation-induced graft polymerization [58, 56, 17]. We published the first successful single-step synthesis of copolymeric $CO_2$ sorbents through RIGP, but our low monomer attachment precluded high $CO_2$ capacity [17]. In this chapter, we report the fabrication of allylamine and diallylamine grafted onto PET and Nylon using peroxide and nitroxide initiators. Chemically initiated graft polymerization (CIGP) offers several advantages over RIGP, namely in total environmental cost of energy for radicalization and relative ease of grafting procedure. We also discuss characterization of monomer attachment through gravimetric analysis, FTIR, and EDX.

## 4.2 Methodology of Peroxide and Nitroxide-Induced Grafting

While radiation-induced grafting provides better control in terms of radiation dose and procedure, it causes relatively low radical yield as discussed in previously published literature [47, 46]. We explored chemical-induced grafting using peroxides and nitroxides as a potential alternative, so as to increase $CO_2$ capacity while retaining a digestible, effective grafting procedure.

Benzoyl peroxide and (2,2,6,6-Tetramethylpiperidin-1-yl)oxyl (TEMPO) were explored as initiators for chemical-induced graft polymerization. Dissociation of such initiators creates the primary free radical species of $C_6H_5COO^\bullet$ and/or the secondary free radical species of $C_6H_5^\bullet$ during polymerization. Through hydrogen abstraction, these primary and secondary free radical species form carbon-centered PET macroradicals, like those obtained through radiation. The free radical on the PET attacks the vinyl group of the monomers, creating a sigma bond and unpaired electrons. After this first propagation step, more monomers continue to bind onto the growing grafted polymer chain.

Following the same preprocessing procedure as in section 3.2.3, 50-mg square swatches of PET and Nylon-6 fabric were refluxed in THF to remove the protective polylactic acid coating. To begin, we first dissolved the initiators: benzoyl peroxide in toluene and TEMPO in ethanol, at 10-20 wt. % and 5-10 % respectively. These ratios followed closely with those of literature [46]. Approximately 5 mL of each solution were prepared in the 10-mL vials used, filling half the vial. Solutions were thoroughly purged with argon to remove dissolved oxygen, which if present can form unwanted peroxides by reacting with radicals on the polymer backbone. These radicals must remain available for our intended monomer to polymerize onto. The PET and Nylon fabrics were added into the solutions for 4 hours before removing the solutions from the vials. Afterwards, approximately 10 mL of 100 % monomer solutions of allylamine and diallylamine were introduced to the fabric samples in the vials and the monomers were left to polymerize overnight.

After grafting, potential homopolymers were washed off with several cycles of rinsing, vortexing, and sonication. Rinses were done alternating between water and methanol. Fabrics were then dried in vacuum desiccators and inert atmosphere for storage before $CO_2$ capacity testing.

## 4.3   Results and Discussion

In addition to radiation-induced graft polymerization (RIGP), chemically initiated graft polymerization (CIGP) was also investigated. Benzoyl peroxide as well as nitroxide were each used as radical initiators. The attachment of nitrogenous monomers was charac-

terized gravimetrically via degree of grafting calculation, FTIR spectroscopy, and EDX elemental analysis.

Gravimetrically, CIGP-treated fabrics showed attachment of nitrogen-containing monomer. Figure 19 shows that while many fabrics achieved positive degrees of grafting, there were multiple samples that exhibited negative DoG values. These negative values can be attributed to $\beta$-scission of the fibers' polymer chains, which is a known result of the radicalization of benzoyl peroxide as well as other peroxy derivatives [14]. This scission results in the loss of small fragments of fiber due to post-grafting processing. In addition, the organic and aqueous solvents used swell both nylon and PET, enhancing the probability of fibers entering the solution during post-grafting washes. This loss of fiber mass may have artificially decreased the measured degree of grafting values to levels below 0.
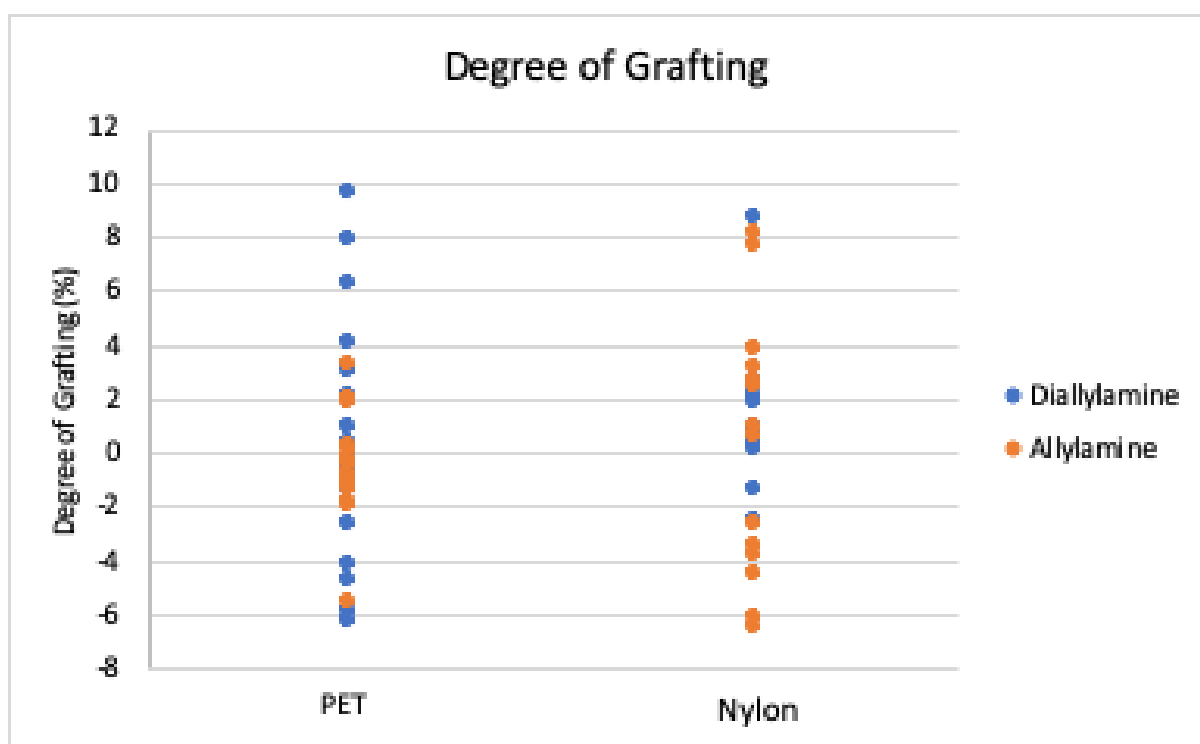


Figure 19: Degree of grafting values for allylamine-grafted (orange) and diallylamine-grafted (blue) PET and Nylon fabrics that have undergone chemically initiated graft polymerization (CIGP) treatment.

Observed using FTIR, characteristic peaks at 764, 1,619, 3,360 and 3,442 cm$^{-1}$ indicate the presence of primary amine functional groups; additionally, the peak at 1,261 cm$^{-1}$ represents the CN stretch that would form between the grafted monomer and the fabric

substrate [8]. Figure 20 also shows the collected FTIR spectra for ungrafted, allylamine-grafted, and diallylamine-grafted fabrics. The Nylon spectra do not show great increase in intensity at the aforementioned peak locations; however, this lack of growth can be attributed to nylon's structure, which already contains amines in great quantity. These amines likely conceal the growth of the characteristic peaks. Although the PET spectra do not show a dramatic increase in any of the characteristic peak intensities, the peak corresponding to the CN stretch did noticeably increase. This increase qualitatively confirms monomer attachment in PET. However, monomer attachment on nylon cannot be confirmed with FTIR alone.
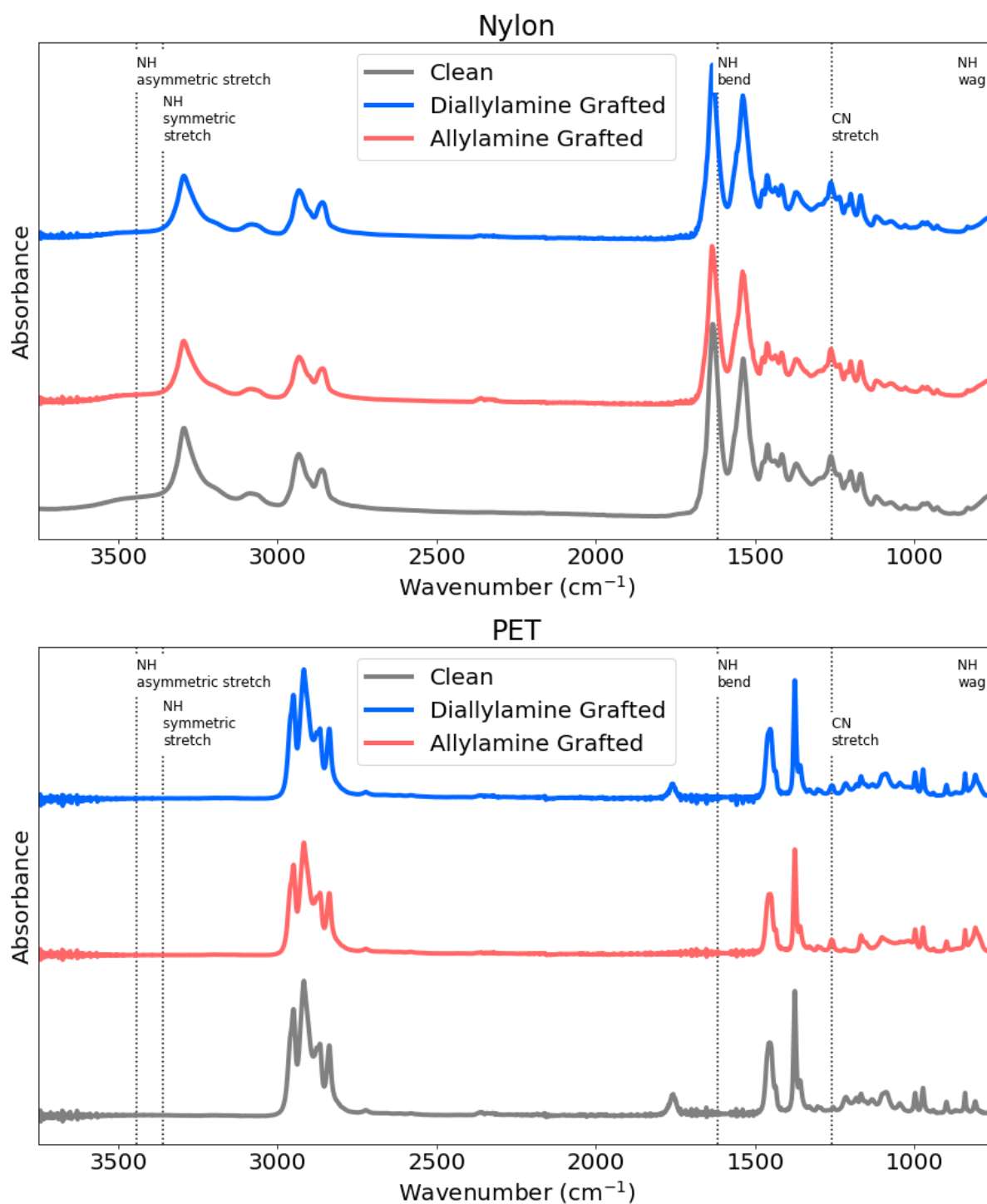
Figure 20: FTIR spectra of ungrafted, allylamine-grafted, and diallylamine-grafted Nylon (top) and PET (bottom).

EDX was also used to confirm monomer attachment. Linescans obtained of both PET and Nylon that underwent CIGP showed that these materials contained higher amounts of nitrogen, which is indicative of successful grafting of nitrogen-containing allylamine and diallylamine. Figure 21 shows the average ratio between nitrogen-attributed and carbon-

attributed X-ray counts for ungrafted, allylamine-grafted, and diallylamine-grafted PET and Nylon samples. The rather high variance in the obtained data can be attributed to the uneven geometry present in fibrous materials, which results in a proportionately uneven spatial emission of X-rays from the sample to the EDX detector. The low signal-to-noise ratio caused by this unevenness likely resulted in such high variance. Nevertheless, the data show an increase in nitrogen content in the analyzed grafted samples.
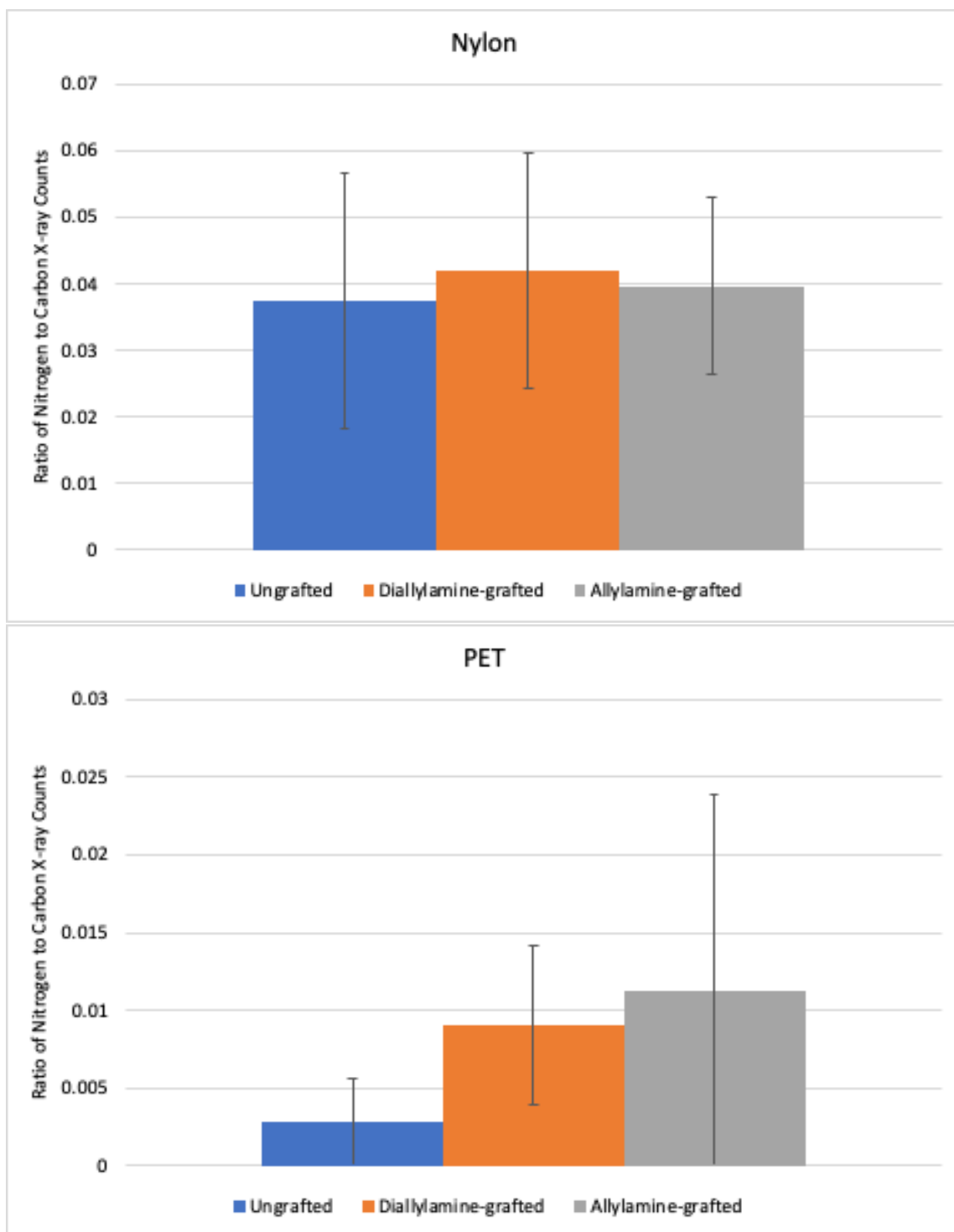
Figure 21: EDS-obtained ratios between nitrogen-attributed and carbon-attributed X-ray counts on ungrafted, allylamine-grafted, and diallylamine-grafted PET and Nylon.

The degrees of grafting for the samples used in the EDX and FTIR analyses are shown in Table 5 below. Specifically, samples with low DoG values were analyzed with EDX to demonstrate that even fabrics with gravimetrically low attachment of monomer still exhibit higher nitrogen content than ungrafted samples, thus indicating successful

grafting.

| | DoG (%) | |
| | Diallylamine | Allylamine |
| --- | --- | --- |
| PET | 2.08 | 0.66 |
| Nylon | 0.21 | 8.14 |

Table 5: Degree of grafting values for samples analyzed via EDS and FTIR

## 4.4 Conclusions on Comparing Radiation Induced and Chemical-Initiated Graft Polymerization

Chemically initiated graft polymerization (CIGP) offers several advantages as compared to RIGP, specifically with respect to throughput of sorbents and environmental impact of the synthesis process. Our successful development of a single-step RIGP process required the use of an electron beam capable of outputting 10 MeV electrons and delivering 250 kGy of total dose [17]. This equipment is expensive, difficult to obtain, and requires high energy costs. Thus, CIGP-driven synthesis lowers the barrier to commercial or research production of the novel $CO_2$ sorbents reported here. In addition, the nitroxide initiator used is soluble in water and ethanol, two environmentally friendly solvent. Thus, the CIGP procedure described in this chapter enables environmentally-friendly synthesis of $CO_2$ sorbents.

Both RIGP and CIGP reactions are highly vulnerable to peroxide formation; an undesired reaction in which molecular oxygen in the atmosphere or solution reacts with a radical on the polymer backbone to form peroxide. Peroxide formation eliminates backbone-centered radicals necessary for grafting. We performed CIGP with ethanol as the solvent for nitroxides; given the high solubility of molecular oxygen in ethanol, which has an Oswald distribution value of 0.233, preventing peroxide formation from inhibiting graft polymerization posed a considerable challenge [2]. Despite using a glovebox to perform reactions in an inert atmosphere and sparging of solvents with argon, we still achieved far less grafting with CIGP when compared to that of RIGP. Though we achieved approximately 17 % DoG with RIGP, we could only achieve 9 % DoG with CIGP. Effective application of CIGP to fabricating $CO_2$ sorbents therefore requires extreme caution

to prevent molecular oxygen from suppressing grafting. CIGP also poses specific challenges with respect to characterization. Gravimetric analysis, which produced the degree of grafting measure commonly used to assess monomer attachment in graft polymerization, may lose accuracy in chemically initiated copolymers [13, 17]. Gravimetric analysis relies on the assumption that any change in mass stems from added monomer. However, the initiating solvent used in CIGP typically swells the polymer, potentially removing fibers from the fabrics. This would decrease the mass of the fabrics, artificially lowering the measured DoG. Since Nylon and PET swell to different degrees in ethanol, this effect differs between fabric samples [57].

# 5    Economic and Environmental Analysis

## 5.1    Economic Analysis

In the economic analysis of the synthesis of carbon capturing fabrics, four main aspects were considered: cost of initiation, cost of monomers, cost of fabric, and cost of $CO_2$ removal. The cost of initiating the polymerization was considered using the electricity cost associated with the electron beam or the cost of chemical initiators. The capital cost of the electron beam is \$300,000-\$500,000; however, this cost was neglected for this analysis because, in the long run, a net positive operating cost will overcome the capital cost and the electron beam can be used for other tasks. The bulk cost of amine-based monomers, chemical initiators, and fabrics were obtained from sources online including Sigma-Aldrich and ICIS; however, these costs are likely higher than the minimum purchasing cost [69, 70, 71, 72, 73, 74]. The steam was assumed to be the more expensive high pressure steam, and the cost was determined from Warren Seider's chemical process design textbook [49].

The masses of monomer and chemical initiator needed to synthesize the fabric were assumed to be equal to 5 times the mass of the fabric, similar to the ratios used in our chemical grafting procedure. This assumption is reasonable because the amount of monomer grafted to each sample is certainly less than the initial mass of the fabric, and,

even when optimized, not all of the substrate will initiate. The amount of steam required to remove a mmol of $CO_2$ from the fabric was determined by equation (6).

$$M_{SteamRemoval} = (\delta_{CO_2}(SatWater))(mmolFactor) \tag{6}$$

Equation (7) gives the total operating cost normalized per gram of fabric.

$$Cost_{operating} = Cost_{Initiation} + Cost_{Monomer} + Cost_{Fabric} + n(Cost_{Steam})(SC)(Cap_{CO_2}) \tag{7}$$

Furthermore, as shown in Table 6-8, the mass of fabric required to capture one ton of $CO_2$ is calculated by equation (8).

$$Mass_{Ton,CO_2} = \frac{22730000}{n(Capacity)} \tag{8}$$

The operating cost can be leveraged along with the capacity to determine the cost of capturing one ton of $CO_2$. The monetary cost to capture one ton of $CO_2$ is calculated with equation (9)

$$Cost_{Ton,CO_2} = Cost_{Operating}(Mass_{Ton,CO_2}) \tag{9}$$

Ideally, the cost per ton of $CO_2$ captured is between \$100 and \$350 in order to maintain economic viability based upon the market price of captured $CO_2$ [44].

## 5.2  Environmental Analysis

In preliminary assessments of the functionalized fabrics, both radiation and chemically initiated grafting yielded minor, yet promising, results in terms of environmental impact. Evaluating the net environmental effect of the functionalized fabrics requires assessment of the energy used to radicalize the fabric and the $CO_2$ captured by the fabric over time.

To quantify the environmental impact of energy used to radicalize the fabrics, this study calculated the equivalent $CO_2$ emissions necessary to produce the energy required. Because the peroxide-induced and nitroxide-induced grafting procedure only requires thorough mixing of peroxides, nitroxides, fabric, solvents, and monomers, there were

no direct sources of $CO_2$ emissions. Radiation-induced grafting requires the use of an e-beam, however. The energy to operate the beam at the required dose of 5.56 x $10^{-5}$ kWh per gram fabric translates to an approximate 0.566 mmol $CO_2$ emitted per gram fabric.

The synthesized fabrics can only be effective at addressing climate change if the $CO_2$ emitted in production is offset by the $CO_2$ captured during the lifetime of the fabric. Net $CO_2$ sequestration is calculated with equation (10).

$$NetCO_2Sequestration = n(Capacity) - Emissions \qquad (10)$$

Table 6: Economic and environmental analyses of one-time use of the functionalized fabric at experimentally-derived $CO_2$ capacities. The best monomer-substrate combinations are evaluated at each radicalization method, with radiation being on allylamine-PET, peroxide on diallylamine-Nylon, and nitroxide also being on diallylamine-Nylon.

|  | Radiation | Peroxide | Nitroxide |
|---|---|---|---|
| Net $CO_2$ Sequestration (mmol $CO_2$/g fabric) | -0.566 | $2.48 \times 10^{-5}$ | $5.19 \times 10^{-4}$ |
| Total Operating Cost ($/g fabric) | 0.497 | 2.09 | 32.40 |
| Functionalized Fabric Required to Capture One Ton of $CO_2$ (g fabric) | $5.17 \times 10^{10}$ | $9.18 \times 10^{11}$ | $4.38 \times 10^{10}$ |
| Cost per Ton of $CO_2$ captured | $2.57 \times 10^{10}$ | $1.92 \times 10^{12}$ | $1.42 \times 10^{12}$ |

Table 7: Economic and environmental analyses of extended use (50 cycles) of the functionalized fabric at experimentally-derived $CO_2$ capacities. The best monomer-substrate combinations are evaluated at each radicalization method, with radiation being on allylamine-PET, peroxide on diallylamine-Nylon, and nitroxide also being on diallylamine-Nylon

|  | Radiation | Peroxide | Nitroxide |
|---|---|---|---|
| Net $CO_2$ Sequestration (mmol $CO_2$/g fabric) | -0.544 | $1.24 \times 10^{-3}$ | 0.0259 |
| Total Operating Cost ($/g fabric) | 0.497 | 2.09 | 32.40 |
| Functionalized Fabric Required to Capture One Ton of $CO_2$ (g fabric) | $1.03 \times 10^9$ | $1.84 \times 10^{10}$ | $8.76 \times 10^8$ |
| Cost per Ton of $CO_2$ captured | $5.14 \times 10^8$ | $3.84 \times 10^{10}$ | $2.48 \times 10^{10}$ |

Table 8: Economic and environmental analyses of one-time use of the functionalized fabric at a theoretical $CO_2$ capacity of 2 mmol/g. The best monomer-substrate combination of allylamine-PET is shown.

|  | Radiation |
|---|---|
| $CO_2$ Capacity Required to Sell One Ton of $CO_2$ for $100 (mmol/g fabric) | $2.30 \times 10^4$ |
| Total Operating Cost ($/g fabric) | 0.502 |
| Functionalized Fabric Required to Capture One Ton of $CO_2$ (g fabric) | $1.14 \times 10^7$ |
| Cost per Ton of $CO_2$ captured | $5.71 \times 10^6$ |

Table 9: Economic and environmental analyses of extended use (50 cycles) of the functionalized fabric at a theoretical $CO_2$ capacity of 2 mmol/g. The best monomer-substrate combinations of allylamine-PET is shown

| | Radiation |
|---|---|
| $CO_2$ Capacity Required to Sell One Ton of $CO_2$ for \$100 (mmol/g fabric) | $3.36 \times 10^3$ |
| Total Operating Cost (\$/g fabric) | 0.739 |
| Functionalized Fabric Required to Capture One Ton of $CO_2$ (g fabric) | $2.27 \times 10^5$ |
| Cost per Ton of $CO_2$ captured | $1.68 \times 10^5$ |

Radiation-induced polymerization requires much more energy than chemically initiated does due to the electron beam usage. In this analysis, the energy used for performing the chemical synthesis was neglected due to its relatively low magnitude. Due to the higher energy usage, radiation-induced grafting produces more $CO_2$ per gram of fabric, which must be overcome by a larger $CO_2$ capacity. To offset the emissions specifically, a gram of fabric must be able to capture more than 0.566 mmol of $CO_2$ over its lifetime.

Fabrics created through CIGP can afford to have a slightly lower capacity; however, the production cost per gram of fabric of CIGP is much greater than that of RIGP. This higher cost makes it much more difficult to achieve the economic viability threshold of \$100 per ton of $CO_2$ captured. As indicated in Table 9, at the specified operating cost and assuming a capacity of 2 mmol/g and 50 stripping cycles, the removal of a ton of $CO_2$ from the atmosphere would require \$168,000 using radiation and \$7.42 million using nitroxides. This result indicates that radiation-induced grafting has greater economic potential so long as it can achieve the capacity required.

Based upon the gathered data, the maximum capacity of peroxides is much lower than that achieved by nitroxides and therefore the peroxide method is less cost-efficient despite its lower cost per gram. With \$100, 135 g of fabric can be generated through RIGP when the fabric undergoes 50 cycles of steam stripping. With the same cost limitations, only 3 g can be generated when put through 50 steam stripping cycles with nitroxide grafting. As a result, to capture one ton of $CO_2$ at a cost of \$100 with the calculated operating cost, the capacity must be 3,358 mmol/g for radiation-grafting and 148,406 mmol/g using nitroxide grafting. These capacities are much greater than those achieved by other carbon capture methods; therefore, the \$100 per ton of $CO_2$ goal can only be achieved

through a combination of improving $CO_2$ capacity, extending the life cycle of each fabric, and reducing operating costs.

# 6 Conclusion

## 6.1 Comparison Between CIGP and RIGP

Both chemically initiated and radiation-induced graft polymerization offer distinct advantages when looking to synthesize a graft copolymer for $CO_2$ extraction. The methods for chemical initiation discussed in this study only requires the mixing of chemicals, so no $CO_2$ is produced in order to initiate radicals on our fabrics. Conversely, the operation of an electron beam requires the emission of $CO_2$. In order to become a truly carbon negative option for sequestration, the fabrics must feature a high $CO_2$ capacity to overcome this barrier from electron beam operation.

Due to this, chemically initiated graft polymerization can afford to have a slightly lower capacity due to its lack of $CO_2$ emissions. Unfortunately, production costs for the synthesis of a fabric produced through CIGP are significantly higher than those produced through RIGP. Specifically, as shown in Table 9, the cost per ton of $CO_2$ removed from the atmosphere is much lower for RIGP fabrics than CIGP fabrics. As a result, we can conclude that radiation grafting has a greater economic potential so long as it can achieve the $CO_2$ capacities required to overcome the barrier produced by the electron beam operation.

Each of these methods also offer benefits and drawbacks in terms of their accessibility and ease of operation. RIGP requires the use of an electron beam or alternative radiation source, which can require costly reservations. However, CIGP only requires the mixing of chemicals, so the synthesis can be performed in any available fume hood. Additionally, all of the chemicals used in CIGP to initiate the fabric are water/ethanol soluble, allowing for an environmentally friendly synthesis of a $CO_2$ sorbent. Unfortunately, our ability to characterize our CIGP fabrics was limited by the degradation of the fabrics during

initiation. As our fabrics swelled with our peroxide/nitroxide initiator, individual fibers were detached from the fabric, leading to mass loss. This limited the effectiveness of our gravimetric analysis, which served as one of the main quantitative measures in this study. Conversely, as depicted in Figure 12, there is little to no degradation shown in the fabrics produced through RIGP, allowing for the use of gravimetric analysis as a quantitative measure of monomer attachment to the backbone.

## 6.2   Uses for Captured $CO_2$

While outside the scope of our research, investigating the use of captured carbon provides understanding of the financial in addition to environmental benefits. In section 5, a competitive price of $100 per gallon of sequestered $CO_2$ is used for calculations, but more detailed insight on the usage leads us to believe that the market for captured carbon adds incentive for those researching methods of $CO_2$ capture.

Captured aqueous carbon has risen in commercial value as society begins to develop methods of using it. Enhanced oil recovery (EOR) serves as the most prominent use of captured $CO_2$. Injecting $CO_2$ into oil fields decreases the viscosity and increases pressure of the crude oil, allowing for augmented flow [41]. Additionally, 90-95 % of $CO_2$ used remains stored within the land using the closed-loop systems of the EOR facilities. In 1972, when this technique was first implemented, natural gas separation produced $CO_2$, which would then be used for the process. With more recent, effective methods of carbon capture, EOR will remain the dominant use of sequestered $CO_2$ [9, 10]. While the oil industry clearly adds to the climate change problem, the positive implications of $CO_2$ storage within the crude oil fields as well as the boosting of fracking efficiency helps to minimize the negative environmental impact.

Long term storage in deep saline aquifers offers another option for captured carbon. Through injection into very deep water-permeable rock formations, $CO_2$ dissolves within brine and remains geo-chemically trapped for thousands to millions of years [50]. Although researched for as little as a few decades, geo-sequestration provides a permanent solution for the excess $CO_2$ that will be captured during the coming years.

## 6.3   Future Work

The main issues faced with the current grafting methodology were the qualitative measuring of grafting and the relatively low $CO_2$ capacity of the functionalized fabrics. While gravimetric, FTIR, and EDX measurements were qualitatively helpful, they were unable to provide sound quantitative confirmation of attachment. If provided time and access to more surface analysis instruments capable of techniques like X-ray photoelectron spectroscopy (XPS) and Auger electron spectroscopy (AES), we may be able to better quantify attachment of monomers.

Given more time, we would also quantify mechanical properties of the bare and functionalized fabrics. Tensile and degradation testing before and after functionalization will provide insight on long-term viability in a commercial setting. Chemical specificity of the $CO_2$ capture mechanism may also be explored more by conducting tests with $Ar/N_2$ and $Ar/O_2$ gas mixtures and comparing with $Ar/CO_2$ capacity data.

Additionally, the novel single-step synthesis method using RIGP could be further explored given extended use of the NIST electron beam. With more time, we could test higher doses of radiation and potentially improve overall $CO_2$ capacities of the sorbents as a result. To further affirm radicalization, we could also characterize blank irradiations of the substrates with gel permeation chromatography (GPC) analysis.

Another method aside from RIGP and CIGP that exhibits potential is with copolymers. Through introduction of already-formed copolymer chains of primary amines to the commercial-grade fabric with further catalysis, we may form a sorbent with higher $CO_2$ capacity.

# References

[1] Akingbogun, O.; Muhr, L.; Vallieres, C. Capture of Carbon Dioxide by an Ion-Exchange Resin: Influence of Gas Humidity on Capture Mechanisms. *Separation Science and Technology* **2017**, 52 (10), 1761–1767. https://doi.org/10.1080/01496395.2017.1293094.

[2] Battino, R. Oxygen and Ozone: Solubility Data Series; Elsevier, 2015.

[3] Bell, V. L.; Pezdirtz, G. F. Effects of Ionizing Radiation on Linear Aromatic Polyesters. *Journal of Polymer Science: Polymer Chemistry Edition* **1983**, 21 (11), 3083–3092. https://doi.org/10.1002/pol.1983.170211106.

[4] Blauwhoff, P. M. M.; Versteeg, G. F.; Van Swaaij, W. P. M. A Study on the Reaction between $CO_2$ and Alkanolamines in Aqueous Solutions. *Chemical Engineering Science* **1984**, 39 (2), 207–225. https://doi.org/10.1016/0009-2509(84)80021-4.

[5] Cavenati, S.; Grande, C. A.; Rodrigues, A. E. Adsorption Equilibrium of Methane, Carbon Dioxide, and Nitrogen on Zeolite 13X at High Pressures. *Journal of Chemical & Engineering Data* **2004**, 49 (4), 1095–1101. https://doi.org/10.1021/je0498917.

[6] Chiang, Y.-C.; Chen, Y.-J.; Wu, C.-Y. Effect of Relative Humidity on Adsorption Breakthrough of $CO_2$ on Activated Carbon Fibers. *Materials (Basel)* **2017**, 10 (11). https://doi.org/10.3390/ma10111296.

[7] Cho, Y.; Lee, J.-Y.; Bokare, A.; Kwon, S.-B.; Park, D.-S.; Jung, W.-S.; Choi, J.-S.; Yang, Y.-M.; Lee, J.-Y.; Choi, W. LiOH-Embedded Zeolite for Carbon Dioxide Capture under Ambient Conditions. *Journal of Industrial and Engineering Chemistry* **2015**, 22, 350–356.

[8] Craver, C. D. The Coblentz Society Desk Book of Infrared Spectra,; *NATIONAL STANDARD REFERENCE DATA SYSTEM, NATIONAL STANDARD REFERENCE DATA SYSTEM*, **1977**.

[9] Dai, Z.; Middleton, R.; Viswanathan, H.; Fessenden-Rahn, J.; Bauman, J.; Pawar, R.; Lee, S.-Y.; McPherson, B. An Integrated Framework for Optimizing $CO_2$ Sequestration and Enhanced Oil Recovery. *Environmental Science & Technology Letters* **2014**, 1 (1), 49–54. https://doi.org/10.1021/ez4001033.

[10] Dai, Z.; Stauffer, P. H.; Carey, J. W.; Middleton, R. S.; Lu, Z.; Jacobs, J. F.; Hnottavange-Telleen, K.; Spangler, L. H. Pre-Site Characterization Risk Analysis for Commercial-Scale Carbon Sequestration. *Environ. Sci. Technol.* **2014**, 48 (7), 3908–3915. https://doi.org/10.1021/es405468p.

[11] Danckwerts, P. V. The Reaction of $CO_2$ with Ethanolamines. Chemical Engineering Science 1979, 34 (4), 443–446. https://doi.org/10.1016/0009-2509(79)85087-3.

[12] Dietz, T. (ORCID:0000000187333227); Fastow, E.; Tsoi, M.; Tsinas, Z.; Pazos, I.; Al-Sheikhly, M. Enhancement of the Extraction of Uranium from Seawater; DOE-UMD-0008437-1 15-8663; Univ. of Maryland, College Park, MD (United States), 2018. https://doi.org/10.2172/1489218.

[13] Dietz, T. C.; Tomaszewski, C. E.; Tsinas, Z.; Poster, D.; Barkatt, A.; Adel-Hadadi, M.; Bateman, F. B.; Cumberland, L. T.; Schneider, E.; Gaskell, K.; LaVerne, J.; Al-Sheikhly, M. Uranium Removal from Seawater by Means of Polyamide 6 Fibers Directly Grafted with Diallyl Oxalate through a Single-Step, Solvent-Free Irradiation Process. *Industrial & Engineering Chemistry Research* **2016**, 55 (15), 4179–4186. https://doi.org/10.1021/acs.iecr.5b03401.

[14] Diop, M. F.; Torkelson, J. M. Ester Functionalization of Polypropylene via Controlled Decomposition of Benzoyl Peroxide during Solid-State Shear Pulverization. *Macromolecules* **2013**, 46 (19), 7834–7844. https://doi.org/10.1021/ma401628u.

[15] Dole, M. The Radiation Chemistry of Macromolecules; *Elsevier*, **2013**.

[16] Dutcher, B.; Fan, M.; Russell, A. G. Amine-Based $CO_2$ Capture Technology Development from the Beginning of 2013—A Review. *ACS Applied Materials & Interfaces* **2015**, 7 (4), 2137–2148. https://doi.org/10.1021/am507465f.

[17] Fastow, E.; Cook, S.; Dean, P.; Ott, P.; Wilson, J.; Yoon, H.; Dietz, T.; Bateman, F.; Al-Sheikhly, M. Single-Step Synthesis of Atmospheric $CO_2$ Sorbents through Radiation-Induced Graft Polymerization on Commercial-Grade Fabrics. *Radiation Research* **2019**, 192 (2), 219–230. https://doi.org/10.1667/RR15362.1.

[18] Faterpeker, S. A.; Potnis, S. P. Radiation Grafting of Poly(Ethylene Terephthalate)(PET) Fibre, I. Grafting with Vinyl Acetate. *Angew. Makromol. Chem.* **1980**, 90 (1), 69–81. https://doi.org/10.1002/apmc.1980.050900107.

[19] Fisher, J. C.; Tanthana, J.; Chuang, S. S. C. Oxide-Supported Tetraethylenepentamine for $CO_2$ Capture. *Environ. Prog. Sustainable Energy* **2009**, 28 (4), 589–598. https://doi.org/10.1002/ep.10363.

[20] Gholidoust, A.; Atkinson, J. D.; Hashisho, Z. Enhancing $CO_2$ Adsorption via Amine-Impregnated Activated Carbon from Oil Sands Coke. *Energy & Fuels* **2017**, 31 (2), 1756–1763. https://doi.org/10.1021/acs.energyfuels.6b02800.

[21] Hauchhum, L. Carbon Dioxide Adsorption on Zeolites and Activated Carbon by Pressure Swing Adsorption in a Fixed Bed. *International Journal of Energy and Environmental Engineering* **2014**, 5 (4), 349–356. https://doi.org/10.1007/s40095-014-0131-3.

[22] Ho, T. M.; Tuyen, T.; Howes, T.; Bhandari, B. R. Method of Measurement of $CO_2$ Adsorbed into $\alpha$-Cyclodextrin by Infra-Red $CO_2$ Probe. *International Journal of Food Properties* **2016**, 19 (8), 1696–1707. https://doi.org/10.1080/10942912.2015.1084005.

[23] Holland, B. J.; Hay, J. N. The Thermal Degradation of PET and Analogous Polyesters Measured by Thermal Analysis–Fourier Transform Infrared Spectroscopy. *Polymer* **2002**, 43 (6), 1835–1847. https://doi.org/10.1016/S0032-3861(01)00775-3.

[24] House, K. Z.; Baclig, A. C.; Ranjan, M.; Nierop, E. A. van; Wilcox, J.; Herzog, H. J. Economic and Energetic Analysis of Capturing $CO_2$ from Ambient Air. *Proceedings*

*of the National Academy of Sciences of the United States of America* **2011**, 108 (51), 20428–20433. https://doi.org/10.1073/pnas.1012253108.

[25] Islamoglu, T.; Rabbani, M. G.; M. El-Kaderi, H. Impact of Post-Synthesis Modification of Nanoporous Organic Frameworks on Small Gas Uptake and Selective CO 2 Capture. *Journal of Materials Chemistry A* **2013**, 1 (35), 10259–10266. https://doi.org/10.1039/C3TA12305G.

[26] Jackson, P.; Robinson, K.; Puxty, G.; Attalla, M. In Situ Fourier Transform-Infrared (FT-IR) Analysis of Carbon Dioxide Absorption and Desorption in Amine Solutions. *Energy Procedia* **2009**, 1 (1), 985–994. https://doi.org/10.1016/j.egypro.2009.01.131.

[27] Jasso, M.; Krump, H.; Hudec, I.; St'ahel', P.; Kováčik, D.; Šíra, M. Coating of PET Cords at Atmospheric Pressure Plasma Discharge in the Presence of Butadiene/Nitrogen Gas Mixtures. *Surface and Coatings Technology* **2006**, 201 (1), 57–62. https://doi.org/10.1016/j.surfcoat.2005.10.024.

[28] Krimm, S.; Liang, C. Y.; Sutherland, G. B. B. M. Infrared Spectra of High Polymers. II. Polyethylene. *J. Chem. Phys.* **1956**, 25 (3), 549–562. https://doi.org/10.1063/1.1742963.

[29] Lee, S.; Filburn, T. P.; Gray, M.; Park, J.-W.; Song, H.-J. Screening Test of Solid Amine Sorbents for $CO_2$ Capture. *Ind. Eng. Chem. Res.* **2008**, 47 (19), 7419–7423. https://doi.org/10.1021/ie8006984.

[30] Li, W., Choi, S., Drese, J. H., Hornbostel, M., Krishnan, G., Eisenberger, P. M., & Jones, C. W. (2010, June 23). Steam-Stripping for Regeneration of Supported Amine-Based $CO_2$ Adsorbents. Retrieved from https://onlinelibrary.wiley.com/doi/abs/10.1002/cssc.201000131

[31] Li, K.-M.; Jiang, J.-G.; Tian, S.-C.; Chen, X.-J.; Yan, F. Influence of Silica Types on Synthesis and Performance of Amine–Silica Hybrid Materials Used for $CO_2$ Capture. *J. Phys. Chem. C* **2014**, 118 (5), 2454–2462. https://doi.org/10.1021/jp408354r.

[32] Li, P.; Zhang, S.; Chen, S.; Zhang, Q.; Pan, J.; Ge, B. Preparation and Adsorption Properties of Polyethylenimine Containing Fibrous Adsorbent for Carbon Dioxide Capture. *J. Appl. Polym. Sci.* **2008**, 108 (6), 3851–3858. https://doi.org/10.1002/app.27937.

[33] Li, W.; Choi, S.; Drese, J. H.; Hornbostel, M.; Krishnan, G.; Eisenberger, P. M.; Jones, C. W. Steam-Stripping for Regeneration of Supported Amine-Based $CO_2$ Adsorbents. *ChemSusChem* **2010**, 3 (8), 899–903. https://doi.org/10.1002/cssc.201000131.

[34] Liang, C. Y.; Krimm, S. Infrared Spectra of High Polymers. III. Polytetrafluoroethylene and Polychlorotrifluoroethylene. *J. Chem. Phys.* **1956**, 25 (3), 563–571. https://doi.org/10.1063/1.1742964.

[35] Lu, W.; Sculley, J. P.; Yuan, D.; Krishna, R.; Zhou, H.-C. Carbon Dioxide Capture from Air Using Amine-Grafted Porous Polymer Networks. *J. Phys. Chem. C* **2013**, 117 (8), 4057–4061. https://doi.org/10.1021/jp311512q.

[36] Mahajani, V. V.; Joshi, J. B. Kinetics of Reactions between Carbon Dioxide and Alkanolamines. *Gas Separation & Purification* **1988**, 2 (2), 50–64. https://doi.org/10.1016/0950-4214(88)80013-6.

[37] Maschmeyer, T.; van de Water, L. An Overview of Zeolite, Zeotype and Mesoporous Solids Chemistry: Design, Synthesis and Catalytic Properties. Catalysts for Fine Chemical Synthesis: Microporous and Mesoporous Solid Catalysts; Vol. 4, pp 1–38.

[38] Matyjaszewski, K.; Davis, T. P. Handbook of Radical Polymerization; *John Wiley & Sons*, **2003**.

[39] McCann, N.; Maeder, M.; Attalla, M. Simulation of Enthalpy and Capacity of $CO_2$ Absorption by Aqueous Amine Systems. *Ind. Eng. Chem. Res.* **2008**, 47 (6), 2002–2009. https://doi.org/10.1021/ie070619a.

[40] IPCC Special Report on Carbon Dioxide Capture and Storage; Metz, B., Intergovernmental Panel on Climate Change, Eds.; Cambridge University Press, for the Intergovernmental Panel on Climate Change: Cambridge, **2005**.

[41] Melzer, L. S. Carbon Dioxide Enhanced Oil Recovery ($CO_2$ EOR): Factors Involved in Adding Carbon Capture, Utilization and Storage (CCUS) to Enhanced Oil Recovery. *Center for Climate and Energy Solutions* **2012**.

[42] IPCC Special Report on Carbon Dioxide Capture and Storage; Metz, B., Intergovernmental Panel on Climate Change, Eds.; Cambridge University Press, for the Intergovernmental Panel on Climate Change: Cambridge, **2005**.

[43] Nahas, K. A.; Cama, J.; Schaich, M.; Hammond, K.; Deshpande, S.; Dekker, C.; Ryadnov, M. G.; Keyser, U. F. A Microfluidic Platform for the Characterisation of Membrane Active Antimicrobials. *Lab Chip* **2019**, 19 (5), 837–844. https://doi.org/10.1039/C8LC00932E.

[44] Peters, A. (**2019**, June 17). We have the tech to suck $CO_2$ from the air–but can it suck enough to make a difference? Retrieved from https://www.fastcompany.com/90356326/we-have-the-tech-to-suck-$CO_2$-from-the-air-but-can-it-suck-enough-to-make-a-difference

[45] Pinkas, J. CHEMISTRY OF SILICATES AND ALUMINOSILICATES. Ceramics - Silikáty **2005**, 49, 287–298.

[46] Sacak, M.; Celik, M. Hydrogen Peroxide Initiated Grafting of Acrylamide onto Poly(Ethylene Terephthalate) Fibers in Benzyl Alcohol. *J. Appl. Polym. Sci.* **1996**, 59 (7), 1191–1194. https://doi.org/10.1002/(SICI)1097-4628(19960214)59:7¡1191::AID-APP17¿3.0.CO;2-8.

[47] Sacak, M.; Oflaz, F. Benzoyl-Peroxide-Initiated Graft Copolymerization of Poly(Ethylene Terephthalate) Fibers with Acrylic Acid. *J. Appl. Polym. Sci.* **1993**, 50 (11), 1909–1916. https://doi.org/10.1002/app.1993.070501107.

[48] Samanta, A.; Zhao, A.; Shimizu, G. K. H.; Sarkar, P.; Gupta, R. Post-Combustion $CO_2$ Capture Using Solid Sorbents: A Review. *Ind. Eng. Chem. Res.* **2012**, 51 (4), 1438–1463. https://doi.org/10.1021/ie200686q.

[49] Seider, W. Product and Process Design Principles: Synthesis, Analysis and Evaluation, 4th Edition,Wiley

[50] Silva, G. D., Ranjith, P., & Perera, M. Geochemical aspects of $CO_2$ sequestration in deep saline aquifers: A review. **Fuel**, **2015** 155, 128–143. doi: 10.1016/j.fuel.2015.03.045

[51] Thiruvenkatachari, R.; Su, S.; An, H.; Yu, X. X. Post Combustion $CO_2$ Capture by Carbon Fibre Monolithic Adsorbents. *Progress in Energy and Combustion Science* **2009**, 35 (5), 438–455. https://doi.org/10.1016/j.pecs.2009.05.003.

[52] Vaidya, P. D.; Kenig, E. Y. $CO_2$-Alkanolamine Reaction Kinetics: A Review of Recent Studies. *Chem. Eng. Technol.* **2007**, 30 (11), 1467–1474. https://doi.org/10.1002/ceat.200700268.

[53] Vaidya, P. D.; Kenig, E. Y. A Study on $CO_2$ Absorption Kinetics by Aqueous Solutions of N,N-Diethylethanolamine and N-Ethylethanolamine. *Chem. Eng. Technol.* **2009**, 32 (4), 556–563. https://doi.org/10.1002/ceat.200800573.

[54] Wang, J.; Wang, M.; Li, W.; Qiao, W.; Long, D.; Ling, L. Application of Polyethylenimine-Impregnated Solid Adsorbents for Direct Capture of Low-Concentration $CO_2$. *AIChE J.* **2015**, 61 (3), 972–980. https://doi.org/10.1002/aic.14679.

[55] Wayner, D. D. M.; Clark, K. B.; Rauk, A.; Yu, D.; Armstrong, D. A. C-H Bond Dissociation Energies of Alkyl Amines: Radical Structures and Stabilization Energies. *J. Am. Chem. Soc.* **1997**, 119 (38), 8925–8932. https://doi.org/10.1021/ja971365v.

[56] Wu, Q.; Chen, S.; Liu, H. Effect of Surface Chemistry of Polyethyleneimine-Grafted Polypropylene Fiber on Its CO 2 Adsorption. *RSC Advances* **2014**, 4 (52), 27176–27183. https://doi.org/10.1039/C4RA01232A.

[57] Wypych, G. Handbook of Polymers; *Elsevier*, **2016**.

[58] Yang, Y.; Li, H.; Chen, S.; Zhao, Y.; Li, Q. Preparation and Characterization of a Solid Amine Adsorbent for Capturing $CO_2$ by Grafting Allylamine onto PAN Fiber. *Langmuir* **2010**, 26 (17), 13897–13902. https://doi.org/10.1021/la101281v.

[59] Yoshida, K.; Toyoura, K.; Matsunaga, K.; Nakahira, A.; Kurata, H.; Ikuhara, Y.; Sasaki, Y. Atomic Sites and Stability of Cs+ Captured within Zeolitic Nanocavities. *Scientific Reports* **2013**, 3. https://doi.org/10.1038/srep02457.

[60] Yu, C.-H. A Review of $CO_2$ Capture by Absorption and Adsorption. *Aerosol and Air Quality Research* **2012**. https://doi.org/10.4209/aaqr.2012.05.0132.

[61] Yu, Q.; Brilman, D. W. F. Design Strategy for $CO_2$ Adsorption from Ambient Air Using a Supported Amine Based Sorbent in a Fixed Bed Reactor. *Energy Procedia* **2017**, 114 (Supplement C), 6102–6114. https://doi.org/10.1016/j.egypro.2017.03.1747.

[62] Zelenak, V.; Halamova, D.; Gaberova, L.; Bloch, E.; Llewellyn, P. Amine-Modified SBA-12 Mesoporous Silica for Carbon Dioxide Capture: Effect of Amine Basicity on Sorption Properties. *Microporous and Mesoporous Materials* **2008**, 116 (1), 358–364. https://doi.org/10.1016/j.micromeso.2008.04.023.

[63] Zeman, F. Energy and Material Balance of $CO_2$ Capture from Ambient Air. *Environ. Sci. Technol.* **2007**, 41 (21), 7558–7563. https://doi.org/10.1021/es070874m.

[64] Zukal, A.; Kubů, M.; Pastva, J. Two-Dimensional Zeolites: Adsorption of Carbon Dioxide on Pristine Materials and on Materials Modified by Magnesium Oxide. *Journal of $CO_2$ Utilization* **2017**, 21, 9–16. https://doi.org/10.1016/j.jcou.2017.06.013.

[65] Climate Change Overview. International Debates **2009**, 7 (9), 4–7.

[66] The Social Cost of Carbon. https://19january2017snapshot.epa.gov/climatechange/social-cost-carbon-.html (accessed Apr 26, 2020).

[67] 2020 Electricity Rates By State (**Updated Feb 2020**). (2020, February 4). Retrieved from https://paylesspower.com/blog/electric-rates-by-state/

[68] Carbon and Usage Calculation Methods. (n.d.). Retrieved from https://carbonfund.org/calculation-methods/

[69] Linear Accelerator Pricing Guide. (n.d.). Retrieved from https://www.oncologysystems.com/resources/linear-accelerator-guides/used-linac-price

[70] Chemical Profile - NYLON-6 and NYLON-6/6. https://www.icis.com/explore/resources/news/2005/12/02/549810/chemical-profile-nylon-6-and-nylon-6-6/ (accessed Mar 30, 2020).

[71] TEMPO 214000. https://www.sigmaaldrich.com/catalog/product/aldrich/214000?lang=en®ion (accessed Mar 30, 2020).

[72] Luperox® A98, Benzoyl peroxide 179981. https://www.sigmaaldrich.com/catalog/product/sial/17 (accessed Mar 30, 2020).

[73] https://www.alibaba.com/product-detail/POLY-ALLYLAMINE-HYDROCHLORIDE-71550-12- 4-62008872588.html?spm=a2700.7724857.normalList.18.462ed964N (accessed Mar 30, 2020).

[74] https://www.alibaba.com/product-detail/Diallylamine-with-best-price-CAS-124-60705764425.ht ml?spm=a2700.7724857.normalList.25.43e92acbhLupU0 (accessed Mar 30, 2020).